Applied Thermal Engineering 264 (2025) 125312

Contents lists available at ScienceDirect

Applied Thermal Engineering

journal homepage: www.elsevier.com/locate/apthermeng

Research Paper

Exergy analysis and thermodynamic optimization of a bioenergy with carbon capture and storage gas power plant using Monte Carlo simulation of sewage sludge composition ☆

Kamil Stasiak [a,*], Ivar Ståle Ertesvåg [b], Paweł Ziółkowski [a], Dariusz Mikielewicz [a]

[a] Gdańsk University of Technology, Faculty of Mechanical Engineering and Ship Technology, Institute of Energy, 11/12 Gabriela Narutowicza Street, PL-80-233 Gdańsk, Poland

[b] Department of Energy and Process Engineering, NTNU Norwegian University of Science and Technology, Kolbjørn Hejes vei 1b, NO-7491 Trondheim, Norway

ARTICLE INFO

Keywords:
Exergy Analysis
BECCS
Sewage Sludge
Process Simulation
Power Plant
Stochastic
Monte Carlo

ABSTRACT

An exergy analysis is performed on the negative CO_2 emission gas power plant (nCO_2PP), which integrates the fuel preparation, power generation and carbon capture process sections. The cycle is modeled in Aspen Plus coupled with REFPROP, combining deterministic and Monte Carlo stochastic approaches, the latter being a novelty in this work. In all cases studied, the simulations maintain the complex thermodynamic relationships. Exergy losses with areas of potential improvement are identified, while Monte Carlo simulation in Python generates sewage sludge composition, improving cycle realism. In the deterministic approach, the exergies are calculated for a single sewage sludge composition under ambient air conditions with relative humidity of 40 %, 50 % (base case) and 60 % and CO_2 air concentration of 375 ppm, 417 ppm (base case) and 1000 ppm, representing a worst case scenario of CO_2 increase until the year 2100. For the deterministic base case nCO_2PP, the largest exergy losses are observed in the wet combustion chamber (127 kW, 62 % efficiency), gasification process (43 kW, 89 % efficiency), and water condensation in the gas scrubber (43 kW, 87 % efficiency), while the nCO_2PP exergy efficiency, related to the chemical exergy of the sewage sludge, is 33.3 %. Sensitivity analysis on turbine vacuum and spray-ejector condenser suction pressure results in an increase of the nCO_2PP efficiency by 0.3 % to 33.6 %. Monte Carlo results are incorporated into the Aspen Plus model after the base case optimization. These yield in a range of nCO_2PP exergy efficiencies from 33.6 % to 39.7 % with a mean of 37.5 %.

1. Introduction

The negative CO_2 emission gas power plant (nCO_2PP) shown in Fig. 1 is the subject of intensive research in a project dedicated to the disposal of sewage sludge with simultaneous generation of electricity and CO_2 capture [1]. The nCO_2PP cycle has already been described in several articles [2–5], as it offers the hope of simultaneously disposing of the harmful products of human activity (e.g. sewage sludge), then allowing the production of useful electricity, and finally allowing the capture of carbon dioxide in a dedicated part of carbon capture and storage (CCS). A contribution to this field has been made in [6], where an exergy analysis of the nCO_2PP system was conducted, investigating aspects of energy efficiency and CO_2 capture. The basic equipment includes: the working medium generator – i.e. the novel wet combustion chamber (WCC) [7,8], the steam-gas expander (GT + GT^{bap}), the novel spray-ejector condenser (SEC) [9,10] and the gasifier [2] in which the sewage sludge is converted into syngas by means of a converter, which is a bleed stream (Fig. 1.). Other equipment includes oxygen, fuel and CO_2 compressors, water pumps and heat exchangers. It is extremely important not only to experimentally test syngas production, but also to correctly include the gasification process in the model to show its contribution to the energy conversion chain.

For a more detailed analysis of the nCO_2PP cycle, it should be noted that sewage sludge enters the gasifier reactor (R) as a feedstock. In addition, a gasifying converter in the form of steam mixed with CO_2 from the turbine bleed, referred to as 0^R, enters R as a feedstock. The gasification reactions take place in R and produce the syngas, which has

☆ This article is part of a special issue entitled: 'ECOS2023' published in Applied Thermal Engineering.

* Corresponding author.
E-mail addresses: kamil.stasiak@pg.edu.pl (K. Stasiak), ivar.s.ertesvag@ntnu.no (I.S. Ertesvåg), pawel.ziolkowski1@pg.edu.pl (P. Ziółkowski), dariusz.mikielewicz@pg.edu.pl (D. Mikielewicz).

https://doi.org/10.1016/j.applthermaleng.2024.125312
Received 7 June 2024; Received in revised form 9 December 2024; Accepted 22 December 2024
Available online 25 December 2024

Nomenclature

E	flow exergy rate, kW
E_d	exergy destruction rate, kW
$\bar{e}$	specific molar exergy, kJ/kmol
$\dot{m}$	mass flow rate, g/s
p	pressure, bar
RH	air relative humidity, %
t	temperature, °C
W	work rate (power), kW

Greek symbols

η	efficiency

Subscripts and superscripts

aCO_2	CO_2 in atmospheric air
Aspen	derived from Aspen Plus
ch	chemical
ex	exergetic
fuel, in	either sewage sludge or producer gas input to the power plant system
nCO_2PP	negative CO_2 emission gas power plant project
O_2, in	oxygen input to the power plant system
rev	reversible
th	thermomechanical
tot	total

different compositions due to the different sludge feedstock compositions modeled later in this paper by the Monte Carlo method and is denoted by point 2^R in Fig. 1. Further downstream, the producer gas is purged of water and nitrogen and sulfur compounds, resulting in a syngas mixture that is fed to the C_{Fuel} compressor and further down the fuel line directly to the WCC. The oxygen, after being produced from the air in the ASU, is sent to the compressor that feeds the WCC [11]. In the WCC there is oxy-combustion of syngas with direct water injection, here oxy-combustion is a type of CO_2 capture method. The exhaust gas is fed to the turbine unit (GT + GT^{bap}). The palisades of the turbine unit, together with the geometry of the flow system, have been presented in a paper [12], which confirmed that it should be designed with high speed, two-stage expansion and bleed. The water injected into the WCC is heated by the exhaust in HE1, which is after the turbine, and partially by the waste heat in the CO_2 capture island, and pressurized to the appropriate level by two pumps in series, $P_{H2O\text{-}WCC}$ and auxiliary $P_{H2O\text{-}WCC}$. After cooling in the regenerative heat exchanger (HE1), the SEC receives the exhaust mixture of reworked steam and CO_2, where the steam condenses, allowing CO_2 capture. The SEC is driven by pressurized motive fluid water via a P_{SEC} pump. After the SEC, the CO_2 is separated from the water by either a cyclone separator or a T-type system and the separated water is returned to the WCC and the excess is discharged from the system. In the final part of the cycle, after separation, the CO_2 enters a system of compressors and is pressurized into the storage tank (ST).

The nCO_2PP cycle is consistent with the idea of a bioenergy with a carbon capture and storage (BECCS) power cycle. This involves using a renewable energy source in the form of biomass in combustion processes and then capturing the carbon dioxide produced in this way, ultimately achieving negative CO_2 emissions. However, in addition to carbon performance, an important parameter for the sustainable conversion of fuel energy is exergy destruction. One of the critical parameters influencing exergy destruction are ambient parameters such as temperature, humidity and pressure, which have already been classified in many works by some well-known authors on the subject [13,14]. It is worth noting that the effect of CO_2 in the air is also beginning to play an increasingly important role in exergy analyses, while the issue of determining the chemical exergy of individual elements still lacks a sufficiently reliable physical basis, and most scholars rely on Szargut [14] in this area. The situation is even more complicated when determining the chemical exergy of different types of biomass [15]. First of all, there is a lack of a clear chemical and physical foundation to move from well-established methods to determine the composition of the

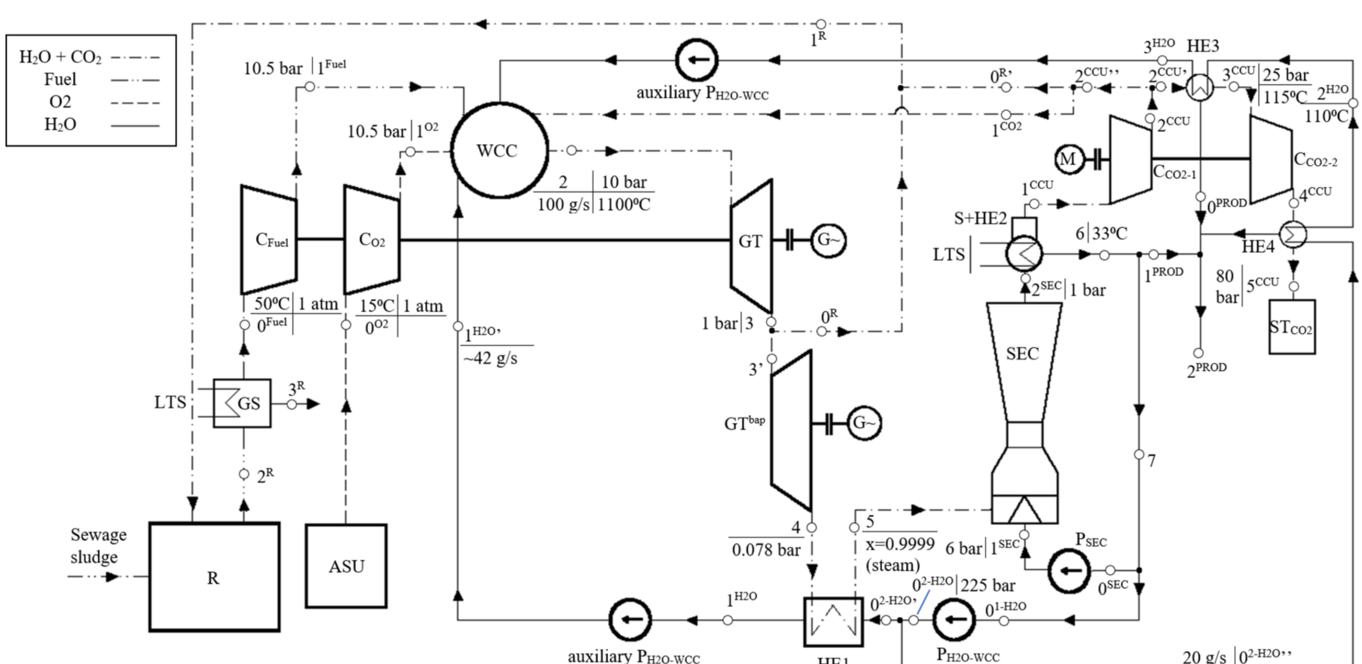

Fig. 1. nCO_2PP process flow diagram [5] where main devices are: WCC – wet combustion chamber, GT – gas turbine, GT^{bap} – low-pressure turbine, R – gasifier, SEC – spray-ejector condenser. Additional devices includes: C_{O2} – oxygen compressor, C_{fuel} – fuel compressor, HE1 – heat exchanger 1, G – generator, $P_{H2O\text{-}WCC}$ – WCC water pump, P_{SEC} – SEC pump, S + HE2 – separator connected with heat exchanger 2, $C_{CO2\text{-}1}$ and $C_{CO2\text{-}2}$ – CO_2 compressors, HE3 – heat exchanger 3, HE4 – heat exchanger 4, GS – gas scrubber, ASU – air separation unit, LTS – lower temperature source.

ultimate and proximate type to the exergy, because here, entropy relating to the atomic level plays a role [16]. In the case of the present work, the analyses will focus on a significantly challenging biomass, which is sewage sludge. Attempts to model this process appropriately are being developed particularly intensively in the Aspen Plus environment, where, using mass, momentum and energy balance and the entropy production equation, the exergy destruction due to gasification can be determined [17]. Using these models, it is important to determine the components of the syngas at the reactor outlet and the input supplied to the gasifier. Due to the varying composition of sewage sludge, depending on the region of the world, the calorific value of the sludge and thus, the exergy that is stored in it, also changes [18].

The production of fuel from sewage sludge is closely related to changing the composition of the resulting syngas, and so far such systems as gas microturbines and high-temperature fuel cells, compression ignition engines, and spark ignition engines have been presented in the literature [19–21] as capable of fuel switching.

In addition, there is great hope for the production of alternative fuels using sewage sludge, where exergetic analyses supplement information on the quality of energy conversion to useful products such as hydrogen [22] or methanol [23].

With respect to exergetic efficiency, it is possible to provide feedback on sustainable energy conversion. This is because it is necessary to identify possible ways of reducing the destruction of exergy, especially in devices where an alternative solution can be proposed.

So far, exergetic analyses have been introduced in various types of new systems such as adiabatic CAES [24], air and liquid energy storage systems [25], for the Allam cycle [26], hybrid systems with heat pumps and organic Rankine cycles (oRc) [27].

In the case of the oxy-fuel cycle, which is the subject of this study, it is also important to determine the impact of exergy destruction in the separation processes such as an ASU and a separator such as the SEC. Industrial ASUs rely on cryogenic methods to supply the required amount of oxygen, and methods to reduce power consumption are also found in this part of the system [28]. Thus, exergetic analyses undoubtedly provide an opportunity to study technical and environmental aspects related to energy systems [29]. Therefore, this approach was chosen to analyze the nCO_2PP cycle integrated with syngas production in the sludge gasification process.

Insight into the theoretical operation of a power plant through

Table 1
Review of modeling approaches for BECCS and similar systems.

References	Simulation tool	System configuration	Deterministic vs. stochastic approach	System exergy efficiency
This work –	Aspen Plus with REFPROP for the cycle and Redlich-Kwong-Soave eqaution of state (EoS) for gasification. Python for Monte Carlo stochastic modeling.	BECCS (nCO_2PP) with sewage sludge-fueled oxy-combustion gas-steam turbine. Stochastic cases improved over base case with bleed turbine directed to gasification, partial waste heat from gas scrubber utilization, optimized SEC suction pressure.	Stochastic – various sewage sludge fuel compositions, where bleed exhaust of various compositions is having real effect on gasification. Deterministic – changing exergy dead state humidity and CO_2 in ambient air. Parametric analysis of SEC suction pressure (turbine vacuum).	Base case: 33.0–33.6 %, improved stochastic cases: 33.6–39.7 % with a mean of 37.5 %.
Ertesvåg et al. [6]	Ebsilon software.	BECCS similar to this work (nCO_2PP), except gasification is not included, different scale, and some different minor assumptions.	Deterministic – one syngas fuel and natural gas, changing ambient temperature in dead state. Simple parametric analysis of WCC, SEC, HE2 temperature and pressure, omitting some cycle assumptions such as non-constant exhaust mass flow or no effect of bleed exhaust composition on gasification.	39.3 % (without gasification step)
Kang et al. [30]	Aspen Plus with Peng-Robinson EoS for cycle and STEAM-TA table for water.	Combined heat and power (CHP) consisting of a gas turbine combined with a heat pump fueled by natural gas.	Deterministic – natural gas fuel has uniform composition (pure methane). Parametric analysis of a high temperature heat pump.	22.6 %
Yang et al.[31]	Aspen Plus with Peng-Robinson EoS for oRc. Equilibrium gasification model. Semi-empirical fuel cell model.	CHP consisting of a fuel cell combined with oRc fueled by food waste.	Deterministic – although food waste is used. Gasifier and fuel cell are simulated in parametric analysis.	61.3 %
Samanta and Roy [32]	Aspen Plus with Peng-Robinson EoS, Cycle-Tempo for cycle modeling. Minitab for optimization.	BECCS fueled by wood based on fuel cell, oRc, steam turbine and air heated turbine.	Deterministic – fuel cell and turbine simulated using parametric analysis. Applied complex optimization using response surface methodology.	47.5 %
Ghiat et al. [33]	Aspen Plus with Peng-Robinson EoS (with Boston modifications) and Electrolyte NRTL with Redlisch-Kwong EoS.	BECCS based on biomass integrated gasification combined cycle (BIGCC) fueled by date pits.	Deterministic with parametric analysis of CCS solvent temperature.	57.2 %
Ebrahimi and Ziabasharhagh [34]	Aspen Plus with Redlich-Kwong-Soave EoS (with Boston modifications) for gasification, Aspen Hysys with Peng-Robinson EoS for cryogenic cycles.	BECCS based on BIGCC with pre-combustion CO_2 capture, electricity, heat and LNG production, fueled by rice husk.	Deterministic.	74.1 %
Han et al. [35]	Aspen Plus with Peng-Robinson EoS (with Boston modifications) for high-temperature processes, ELECNRTL for MEA.	BECCS based on BIGCC with pre-combustion CO_2 capture, fueled by sawdust.	Deterministic with parametric analysis of gasifier and gas turbine. Also compared with post-combustion configuration of the cycle.	38.8 %
Xiang et al. [36]	Aspen Plus with Peng-Robinson EoS.	BECCS based on BIGCC with oxy-fuel combustion CO_2 capture, fueled by unspecified biomass.	Deterministic with parametric analysis of gasification pressure.	31.2 %

exergy analysis provides a framework for improving energy efficiency by identifying and improving areas of highest exergy destruction. The novelty of the present work lies in the application of stochastic analysis, addressing the inherent variability in sewage sludge composition, which is a significant limitation of deterministic approaches. In previous publications, the authors have used Aspen Plus [5] and Ebsilon [6] software to model the power plant and cross-check the simulation for two fuel scenarios, a syngas composition and methane, but in one case the power plant was also simulated in Aspen Hysys as a replica of the Aspen Plus model due to its similarity [3]. The introduction of the use of Monte Carlo simulations in this study reduces the uncertainty and provides a more realistic representation of the power plant under varying fuel compositions.

The comparisons with other selected representative studies in Table 1 demonstrate the need to address this research gap. The table provides an overview of the works related to BECCS exergy analyses by simulation tools used, system configurations, type of approach (deterministic vs. stochastic), and exergy efficiency of the systems studied.

The research gap lies in the limited use of stochastic modeling in previous exergy analysis studies of BECCS or similar systems. This work takes a stochastic modeling approach that goes further than previous efforts by also capturing the feedback loop of complex influences such as changing bleed turbine exhaust parameters on gasification or constant combustion mass flow under varying conditions, allowing to capture a more accurate thermodynamic parameters. In addition, unlike most other studies that rely on the widely used Peng-Robinson equation of state, which is often less accurate than experimental results, especially for water and condensed phases [37], this work uses REFPROP, a database of tables and equations of state ranked in the literature for the highest accuracy in calculating thermophysical properties [38]. It should be emphasized that the deterministic parametric approach presented by other papers in Table 1 is essential for identifying parameters to maximize the power plant exergetic efficiency of a BECCS system. However, the papers compared do not analyze fuel variability and often overlook its significant importance. This paper analyzes fuel variability and takes a step forward by doing so stochastically.

2. Methodology

2.1. Principal equations

The flow exergy is usually split into a thermomechanical part and a chemical exergy. The latter consists of a mixing part and the chemical exergy component.

$$E^{\mathrm{tot}} = E^{th} + E^{\mathrm{ch}} \tag{1}$$

The chemical exergy of sewage sludge was calculated as [39]:

$$E_{ss}^{\mathrm{ch}} = \dot{m}_{ss}\cdot LHV_{ss}\frac{1.0412 + 0.2160\cdot\left(\frac{H}{C}\right) - 0.2499\cdot\left(\frac{O}{C}\right)\cdot\left[1 + 0.7884\cdot\left(\frac{H}{C}\right)\right] + 0.0450\cdot\left(\frac{N}{C}\right)}{1 - 0.3035\cdot\left(\frac{O}{C}\right)} \tag{2}$$

where: H/C, O/C, H/C, N/C are mass ratios in the substance. It should be noted, that the formulation in Eq. (2) is made for $O/C < 2.67$. The power plant was simulated using Aspen Plus with the REFPROP (v10.0.0.02) database developed by the National Institute of Standard and Technology (NIST) (cf. Table 2).

A part of the exergy was derived from this software. However, due to the lack of proper documentation of exergy in Aspen software, it was investigated whether this was total exergy, thermomechanical exergy or some part of it. Essentially, the total flow exergy is the reversible work done when a flow is brought into equilibrium with its environment. The "Aspen exergy" is the reversible work done when the flow is brought from the relevant state to the Aspen dead state. Owing to condensation and phase separation when the flow contains H_2O, the mixture is partially separated. This means that the Aspen exergy calculation includes a part of the mixing exergy together with the thermomechanical component. The remaining flow exergy is the reversible work obtained when the flow is brought from the Aspen Plus restricted dead state to equilibrium with the environment [6]:

Table 2
REFPROP (v10.0.0.02) equations of state used [38].

Fluid type / model	Reference	Comments
Water	Wagner, W.; Pruß, A. (2002) [40]	IAPWS-95
Carbon Dioxide	Span, R.; Wagner, W. (1996) [41]	NIST standard
Oxygen	Schmidt, R.; Wagner, W. (1985) [42]	NIST standard
Methane	Setzmann, U.; Wagner, W. (1991) [43]	NIST standard
Carbon Monoxide	Lemmon, E. W.; Span, R. (2006) [44]	NIST standard
Hydrogen	Leachman et al. (2009) [45]	NIST standard
Propane	Lemmon et al. (2009) [38]	NIST standard
Helmholtz mixing model	Kunz et al. (2012) [46]	ISO standard

$$W_{\mathrm{rev}} = T_0\cdot\overline{R}\cdot\left[\sum_{i\neq H_2O} n_i\cdot ln\frac{n_i}{n - n_{H_2O(liq0)}} + \left(n_{H_2O(g0)} + n_{H_2O(liq0)}\right)\cdot ln\frac{p_{s0:H_2O}(T_0)}{p_0}\right] + n_{H_2O(liq0)}\cdot(p_0 - p_{s0})\cdot\overline{v}_{f:H_2O}(T_0) + \sum_i n_i\cdot\overline{e}_i^{\mathrm{ch}} \tag{3}$$

For streams consisting only of liquid water, Eq. (3) reduces to the chemical exergy:

$$W_{\mathrm{rev}} = n_{H_2O(liq0)}\cdot\overline{e}^{\mathrm{ch}}_{H_2O(liq0)} \tag{4}$$

Including the exergy part calculated by Aspen Plus, the total exergy is as follows:

$$E^{\mathrm{tot}} = E^{\mathrm{Aspen}} + W_{\mathrm{rev}} \tag{5}$$

For the purposes of analysis, exergy destruction was obtained from the steady-state exergy balance,

$$E_d = \sum E_{in}^{\mathrm{tot}} - \sum E_{out}^{\mathrm{tot}} + \sum W_{in} - \sum W_{out} \tag{6}$$

The exergy efficiency of a unit is expressed as the outflow-to-inflow ratio of exergy rates,

$$\eta_{ex} = \frac{\sum E_{out}^{\mathrm{tot}} + \sum W_{out}}{\sum E_{in}^{\mathrm{tot}} + \sum W_{in}} \tag{7}$$

A benefit of outflow-to-inflow efficiency (compared to the "task efficiency") is that the efficiency of two or more combined units (subsystems) can be defined simply by the product of the efficiencies of the individual units. The exergy efficiency of the power plant is then expressed as

$$\eta_{ex|nCO_2PP} = \frac{\sum W_{out} - \sum W_{in} + E_{CO_2,out}}{E_{fuel,in} + E_{O_2,in}} \tag{8}$$

Here, to appreciate the CO_2 capture, the thermodynamic value (pressure and chemical exergy) of the captured CO_2 is added.

2.2. Base case input data

For exergy analysis, the Aspen Plus dead state was set to the T_0 temperature of 15°C and p_0 pressure of 1 atm (at sea level 0), which corresponds to most standards. Thus, read values from Aspen Plus with REFPROP equations of state, such as saturation pressure $p_{s0:H_2O}(T_0)$ was 0.0170579 bar and $\overline{v}_{f:H_2O}(T_0)$ was 0.018031 m^3/kmol. The exergy calculation also uses the universal gas constant $\overline{R}$ equal to 8.31433 kJ/(kmol K). The chemical exergy calculations used the composition of dry air [47] based on the US Standard Atmosphere, with the CO_2 concentration assumed to be 375 ppm [13] for the year 2004. For comparison, a global average of 417 ppm was used for the year 2022 [48] and a worst-case scenario of 1000 ppm was predicted for the year 2100 [49]. While varying the relative humidity and CO_2 concentration in the dead state of the exergy analysis, the base case in further study is 50 % relative humidity and 375 ppm CO_2 concentration. Based on the base case, GT^{bap} exhaust pressure / SEC suction pressure (nodes 4 and 5) is analyzed in the context of exergy efficiency.

The composition of the sewage sludge digested in the gasification unit and fueling the whole power plant, was assumed as dry mass fractions 27.9 % C, 6.7 % H, 28.3 % O, 4.4 % N, 0.3 % S, 32.5 % Ash, with 2 % moisture. The synthesis gas produced by gasification in a steam atmosphere (with 3.98 %mol O_2) at 760 °C and, after cleaning in the gas scrubber has a volumetric composition of 9.3 % CO, 46.8 % H_2, 13.9 % CH_4, 26.4 % CO_2 and 3.5 % C_3H_8. Typically, toxic impurities such as tar, nitrogen and sulfur compounds are produced along with the syngas in the producer gas, but their exergy is not included in the calculations because they are removed in the process prior to fueling the power plant and are present in insignificant amounts, and tar formation is not modeled. The thermodynamic cycle assumptions (Table 3) are based on literature sources that are strictly dedicated to a particular part of the system, namely:

- in the context of flow devices such as expanders and compressors, data were used from the work of Chodkiewicz et al. [50],
- in the context of oxyfuel combustion, information was gathered from the work of Anderson et al. [51],
- for the water driven ejector, the operating parameters were taken from the article by Butterworth and Sheer article [52],
- and parameters related to pressure and CO_2 capture method were taken from the work of Ziółkowski et al. [3].

A description of the Eq. (A.1-A.16) used in the energy and exergy balances for the following devices can be found in the Appendix.

Table 3
Assumptions for the thermodynamic cycle.

Parameter	Symbol	Unit	Value
Temperature exhaust after WCC (before GT)	t_2	°C	1100
Mass flow of the exhaust gas from the WCC	$\dot{m}_2$	g/s	100
Exhaust pressure after WCC	p_2	bar	10
Oxygen-fuel excess ratio in WCC	λ	–	1
Initial syngas temperature, after gas scrubber	t_{fuel}	°C	50
Initial oxygen temperature	t_{O2}	°C	15
Syngas fuel pressure before C_{fuel} compressor	p_{0-fuel}	bar	1
Oxygen pressure before C_{O2} compressor	p_{0-O2}	bar	1
Fuel to WCC pressure loss factor	δ_{fuel}	–	0.05
Oxygen to WCC pressure loss factor	δ_{O2}	–	0.05
Regenerative water pressure to WCC	p_{1-H2O}	bar	225
Exhaust vapor quality after HE1	x_5	–	0.999
Exhaust temperature after HE1, before SEC	t_5	°C	33
CO_2 pressure after compressor C_{CCU1}	p_{2-CCU}	bar	25
CO_2 pressure after compressor C_{CCU2}	p_{4-CCU}	bar	80
H_2O temperature after HE4	t_{2-H_2O}	°C	110
CO_2 temperature after HE3	t_{3-CCU}	°C	115
Water vapor from Separator in 1^{CCU} mixed with CO_2 vapor	–	%	100 % humid
Pressure after GT^{bap}, before SEC	p_4	bar	0.078
Temperature after SEC	t_6	°C	35
Turbine GT, internal efficiency (η_i)	η_{iGT}	–	0.89
Turbine GT^{bap},η_i	$\eta_{iGT-bap}$	–	0.89
Fuel compressor C_{fuel},η_i	$\eta_{iC-fuel}$	–	0.87
Oxygen compressor C_{O2},η_i	η_{iC-O2}	–	0.87
WCC water pump $P_{H2O\text{-}WCC}$,η_i	$\eta_{iP-H2O-WCC}$	–	0.8
SEC water pump P_{SEC},η_i	η_{iP-SEC}	–	0.8
CO_2 compressor $C_{CO2\text{-}1}$,η_i	$\eta_{iC-CO2-1}$	–	0.87
CO_2 compressor $C_{CO2\text{-}2}$,η_i	$\eta_{iC-CO2-2}$	–	0.87
Mechanical efficiency for all devices	η_m	–	0.99

2.3. Generation of sewage sludge composition variation for power plant analysis

Current methods used to analyze and model sludge gasification and oxy-combustion processes are often based on limited experimental data, as the composition of sewage sludge varies depending on various factors [2,53]. Insufficient data can lead to errors in the design and optimization of energy systems [54]. This subsection presents a method for generating organic part of sewage sludge compositions (C, H, O, N, S). The chosen method is a Monte Carlo simulation of the multivariate normal distribution, which is commonly used to model stochastic processes and allows the estimation of missing data outcomes [55]. This approach differs from interpolation methods by using randomness, mean, standard deviation, and correlation between variables based on available data with a normal distribution.

The multivariate normal distribution is a vector that is defined as:

$$x \sim \mathrm{N}(\mu, \Sigma) \tag{9}$$

Here, "N" denotes the normal distribution type, where the random vector x is characterized by its mean vector μ and covariance matrix Σ. Specifically:

$$x = (X_1, X_2, \cdots, X_n) \tag{10}$$

where random variables $X_1, X_2, \cdots, X_n$ in our case represent elemental composition (C, H, O, N, S) of the organic part of the sewage sludge.

The mean vector μ is given by:

$$\mu = (E(X_1), E(X_2), \cdots, E(X_n)) \tag{11}$$

where $E(X_i)$ is expected value of X_i.

The covariance matrix Σ

$$\Sigma_i, j = Cov(X_i, X_j) \tag{12}$$

which contains the variances (squared standard deviations) and correlations between the variables.

To generate the artificial sludge compositions, data from 17 experimentally-derived compositions, reported in 15 publications [56–70] previously reviewed by Bora et al. [54], was used. This resulted in the generation of 83 compositions in Python in the study, which together make up 100 compositions for analysis.

Together, the experimental and generated compositions of sewage sludge were subjected to a simulation of gasification in a Gibbs reactor in Aspen Plus software. This resulted in the generation of different syngas compositions, which were calculated using the bleed stream after GT. In contrast to the power plant simulation using the REFPROP equations of state, the Redlich-Kwong-Soave equation of state is used exclusively for the Gibbs reactor due to the presence of solids and compounds not included in REFPROP (Table 2), the rest of the cycle is simulated using REFPROP same as in the base case.

In addition, the following assumptions were made for the purposes of this analysis: the dry sludge ash content was assumed to be 32.5 %, the fixed carbon – 9.4 %, the volatile – 58.1 %, and the moisture – 2 %, respectively, which is consistent with the base case. It should be noted that in the base case, the experimentally derived syngas was used. In order to limit the number of possible Gibbs reactor results to a single one, the gasification agent as bleed stream was assumed to be 0.846 times the required sludge mass flow at the pressure of 1.6 bar, which is similar to the author's study on the modeling of bleed stream gasification [5]. It should be noted that the composition of the bleed stream is subject to change as the flue gas condition changes due to changes in the fuel and water required to maintain the temperature in the WCC. The simulations was performed on the entire power plant model, affecting all units, to maintain key design conditions. These conditions included maintaining the exhaust mass flow at 100 g/s at a temperature of 1100 °C from the WCC. Due to the high exergy loss in the condensation of steam in the gas scrubber, 30 kW of heat transfer rate was assumed to be redirected to the gasification reactor. Another modification was the change of the GT^{bap} exhaust pressure or SEC suction pressure in nodal points 4 and 5 to the pressure corresponding to the highest exergy efficiency obtained for the plant in the sensitivity analysis of the base case.

3. Results and discussion

To complete the exergy analysis, the next step was to calculate the chemical exergy of the sludge and calculate the total exergy and efficiency by substituting the chemical exergies from Table 4 with the Aspen Plus exergy known from the models. Relative humidities of 40 %, 50 % and 60 % were used for the chemical exergy calculations. For comparison, the changing atmospheric CO_2 concentration of 417 ppm for the global near-surface average in 2022 and the worst-case scenario of 1000 ppm predicted for 2100 were added.

The following tables (Tables 5-15) show the change in exergy rates as a function of the change in the dead state parameters. Note that the parameters in Table 3 do not change. The Grassmann exergy flow diagram for the base case (50 % RH, 375 ppm CO_2) is shown in Fig. 2.

For the gasification unit shown in Table 5, the syngas composition results were obtained from the experiment presented in the authors' other work [2]. In this study, some simplifications are applied: the exergy of the ash, nitrogen and sulfur compounds gasification is neglected, focusing only on the most important aspect from the point of view of power generation. Special attention should be given to the high water content in the producer gas and its subsequent treatment in a gas

Table 4
Calculated chemical components exergy in changing air relative humidity or CO_2 concentration according to [13] and based on Szargut model [14].

Parameter	Symbol	Unit	Value				
Relative Humidity	RH	%	40	50	60	50	50
Atmospheric CO_2 concentration	X_{aCO_2}	ppm	375	375	375	417	1000
Chemical exergies of substances	$\bar{e}^{ch}_{O_2}$	kJ/kmol	3762	3766	3770	3766	3773
	$\bar{e}^{ch}_{CO_2}$	kJ/kmol	18,915	18,920	18,924	18,665	16,570
	$\bar{e}^{ch}_{H_2O(liq0)}$	kJ/kmol	2195	1661	1224	1661	1661
	$\bar{e}^{ch}_{H_2O(g0)}$	kJ/kmol	11,980	11,446	11,009	11,446	11,446
	$\bar{e}^{ch}_{H_2}$	kJ/kmol	239,121	238,585	238,146	238,584	238,581
	$\bar{e}^{ch}_{CO}$	kJ/kmol	275,120	275,122	275,124	274,867	272,768
	$\bar{e}^{ch}_{CH_4}$	kJ/kmol	836,442	835,368	834,491	835,113	833,004
	$\bar{e}^{ch}_{C_3H_8}$	kJ/kmol	2,157,893	2,155,747	2,153,991	2,154,981	2,148,661

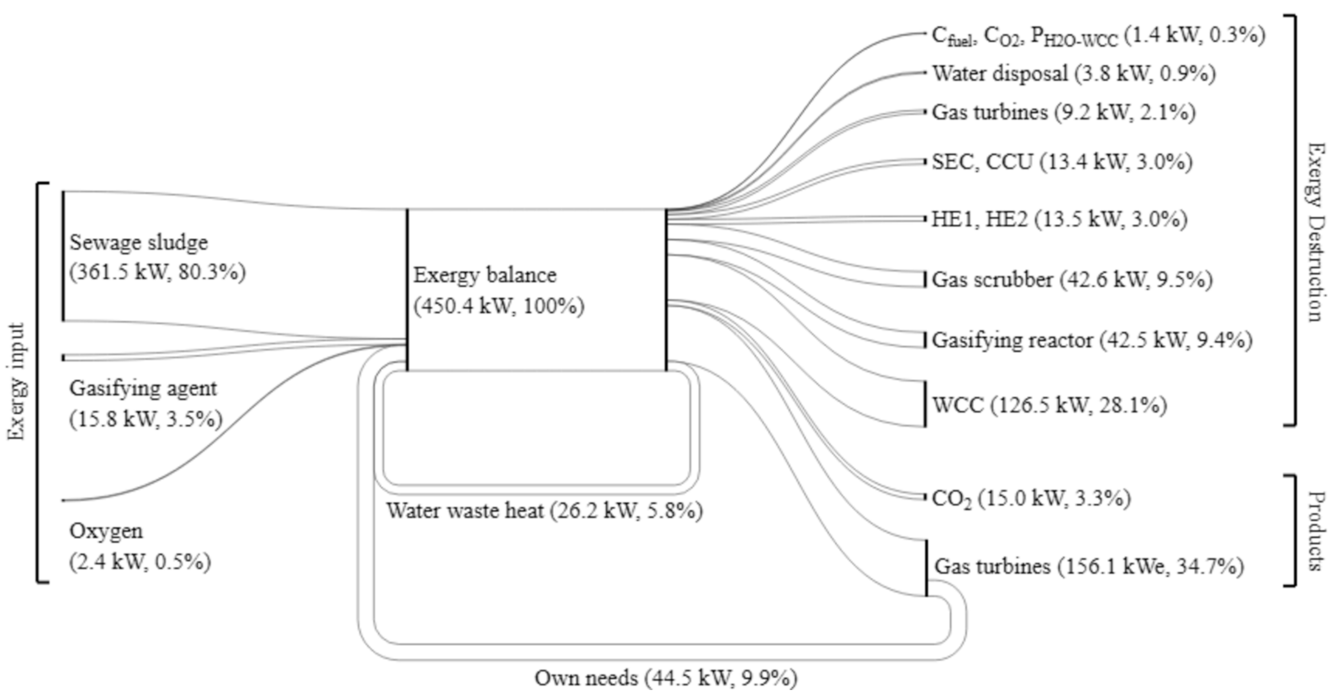

Fig. 2. Grassmann exergy flow diagram of the base case (50 % RH, 375 ppm CO_2) nCO_2PP power plant.

scrubber, whose exergy analysis is shown in Table 6. Using the simplifications mentioned above, the gas scrubber in this case is simply a condenser. While the producer gas has a high temperature, the waste heat can be recovered during the condensation process, which was not foreseen in the nCO_2PP concept as the power plant efficiency of BECCS was usually calculated in the literature without the gasification unit and the gas scrubber and was overlooked, thus opening a way to increase the overall energy efficiency of the power plant. The exergy efficiency of the gasification unit decreases slightly with higher humidity or CO_2 concentration, and the same is true for the gas scrubber. The exergy destructions of these units have some of the highest exergy destructions after the WCC, which are 42–44 kW and 43 kW for the gasification unit and the gas scrubber, respectively. The exergy efficiency of the gasification unit is close to 88–89 %, while that of the gas scrubber is 87 %. The latter can be increased together with the exergy efficiency of the power plant by using the waste heat of water condensation for the power plant processes.

The following points show the exergy rates as a function of the relative humidity and as a function of the CO_2 content in the air. As can be seen from Tables 7 and 8, the variation of the above parameters does not affect the compressors. In the whole range of analyzed parameters, the exergy destruction of the O_2 compressor remains at the level of 0.4 kW, giving an exergy efficiency of 94.7 %, while for the fuel compressor the exergy destruction is 0.6 kW and the exergy efficiency is 99.8 %. It is worth noting that the influence of changing humidity and CO_2 air composition on the exergy destruction of the compressors is reduced to a negligible level due to the absence of H_2O in the compositions of the compressed fluids and the negligible impact of changing the specific chemical exergy of CO_2 in the fuel line. Table 9 applies to water pumps, where the effect of the dead state is much more significant. Despite the constant value of exergy destruction, there is a decrease in exergy efficiency with increasing relative humidity. This is related to the change in the value of the chemical exergy rates carried in the water pumped by the pumps. In contrast, a “task efficiency” would give identical results regardless of the atmospheric composition.

The results for heat exchanger 1 (HE 1) with a heat load of 48.6 kW are shown in Table 10. In this case, the changes in exergy flux are not only for water, but also for the exhaust mixture of water vapor and CO_2. The turbine exhaust flows on one side of the heat exchanger, so the exergy efficiency decreases as both the relative humidity and the fraction of CO_2 in the dead state increase. Again, a “task efficiency” would be independent of the atmospheric composition.

Table 11, which relates to the water-injected oxy-fuel combustor, is of particular interest because it has several functions in this power plant. In addition to producing working fluid with the desired parameters for the gas turbines, it provides oxy-fuel combustion for the carbon capture and utilization (CCU) unit, and it also reuses water that collects waste heat from other parts of the power plant and cools the oxy-fuel flame to the desired temperature. This is why, it is called a ’wet’ combustor. Combustion is assumed to be stoichiometric, with perfect mixing of oxygen and fuel. In reality, some dissociation and kinetics (uncompleted reactions) will result in a somewhat lower adiabatic flame temperature. The exergy destruction rate of this unit is the highest in the whole power plant, about 126 kW, and its exergy efficiency is about 62 %, indicating that special attention needs to be paid to improving this process. With regard to the exergy of the sewage sludge fed into the system, this exergy efficiency would be 49.8 % for the base case when considering the whole process from gasification through water condensation in the gas scrubber, compression and mixing effects in the WCC before ignition and after flame generation, and using the oxygen and H_2O fed into the WCC as direct substrates. It is worth noting that while oxygen mixing with fuel does not cause significant exergy destruction, water mixing into the flame exhaust causes the largest exergy drop in the range of 64–67 kW. Therefore, solutions in the area of water injection into the WCC should be sought to increase efficiency.

Tables 12 and 13 refer to the main useful energy generator, the high-pressure (GT) and low-pressure (GT^{bap}) expander with an output power of 90.4 kW and 65.7 kW, respectively. The total exergy rates are slightly dependent on the amount of CO_2 and the relative humidity of the atmosphere in the dead state. Increasing these parameters results in insignificant changes and virtually no effect on the exergy destruction rates, which were 4.5 kW and 4.8 kW, respectively. In addition, as expected, the gas turbine expanders are characterized by high exergy efficiencies of 97.8 % (GT) and 95.6–95.7 % (GT^{bap}), respectively, at RH = 0.4 and 375 ppm CO_2.

Despite significant exergy rates of about 2730 kW flowing into the SEC, the exergy destruction within this device is 11.3 kW. The value of the exergy efficiency, as shown in Table 14, varies from 99.5 % to 99.7 % in inverse proportion to the increase in relative humidity. It can also be seen that the increase of CO_2 to 1000 ppm in the dead state does not affect the exergy efficiency.

One of the main objectives of the nCO_2PP cycle is to capture carbon dioxide. Therefore, an indispensable part is to determine the exergy conversion in the CCU island, where the following should be distinguished: heat exchangers HE3 and HE4 (heat duty 12.3 kW), compressors $C_{CO2\text{-}1}$ and $C_{CO2\text{-}2}$ (power consumption 10.1 kW). The results of the analysis of the exergy destruction rates and the exergy efficiency are presented in Table 15. It can be seen that for the CCU island there is a clear effect of the amount of CO_2 in the dead state on the exergy efficiency, which decreases from 90.6 % for 375 ppm CO_2 (RH = 0.5) to 89.8 % for 1000 ppm CO_2. This is due to the definition of exergy efficiency, as both inflow and outflow chemical exergies in the numerator and denominator of this formula decrease as atmospheric CO_2 increases. A task efficiency (changed exergy rate by input power) would be unchanged.

3.1. Fuel supply line with gasification process

The results of the exergy analysis of the fuel supply line with the gasification process are presented in Tables 5-7. Table 5 gathers temperature, pressure, mass flow rate and exergy. The established relationships of exergy efficiency and exergy destruction flux indicate their sensitivity to RH and X_{aCO_2} in the gasification unit (R). Another Table 6 shows analogous data collected in terms of heat exchanger of gas scrubber (GS) with heat duty = 112.1 kW. On the other hand, the data for fuel compressor (C_{Fuel}) with mechanical work = 8.5 kW are placed in

Table 5
Gasifying unit (R).

				RH, %	40	50	60	50	50
				X_{aCO_2}, ppm	375	375	375	417	1000
Function	Medium	t, °C	p, bar	$\dot{m}$, g/s	E^{tot}, kW				
Inlet	Sewage Sludge	15	1.013	23.1	361.5	361.5	361.5	361.5	361.5
Inlet	$H_2O(g)$, O_2	100	1.013	27.1	16.8	15.8	15.3	16.0	16.0
Outlet	$H_2O(g)$, CO, CO_2, CH_4, C_3H_8, H_2, without ash	760	1.013	42.2	336.0	334.8	333.8	334.6	333.5
				E_d, kW	42.3	42.5	43.0	42.8	43.9
				η_{ex}, %	88.8	88.7	88.6	88.7	88.4

Table 6
Heat exchanger of Gas Scrubber (GS), Heat Duty = 112.1 kW.

	RH, %				40	50	60	50	50
	X_{aCO_2}, ppm				375	375	375	417	1000
Function	Medium	t, °C	p, bar	$\dot{m}$, g/s	E^{tot}, kW				
Inlet	H_2O(g), CO, CO_2, CH_4, C_3H_8, H_2	760	1.013	42.2	336.0	334.8	333.8	334.6	333.5
Outlet	CO, CO_2, CH_4, C_3H_8, H_2	50	1.013	16.6	290.0	289.6	289.3	289.5	288.4
Outlet	H_2O(liq)	50	1.013	25.6	3.3	2.6	2.0	2.6	2.6
	E_d, kW				42.6	42.6	42.6	42.6	42.6
	η_{ex}, %				87.3	87.3	87.2	87.3	87.2

Table 7
Fuel Compressor (C_{Fuel}), Work = 8.5 kW.

	RH, %				40	50	60	50	50
	X_{aCO_2}, ppm				375	375	375	417	1000
Function	Medium	t, °C	p, bar	$\dot{m}$, g/s	E^{tot}, kW				
Inlet	CO, CO_2, CH_4, C_3H_8, H_2	50	1.013	16.6	290.0	289.6	289.3	289.5	288.4
Outlet	CO, CO_2, CH_4, C_3H_8, H_2	306	10.5	16.6	297.9	297.4	297.1	297.3	296.2
	E_d, kW				0.6	0.6	0.6	0.6	0.6
	η_{ex}, %				99.8	99.8	99.8	99.8	99.8

Table 7. Both parameters of GS and C_{Fuel} do not show a strong relationship with the RH and X_{aCO_2}.

3.2. Oxygen supply line

In the oxygen supply line, one device was singled out, namely the oxygen compressor (C_{O2}), for which data is collected in Table 8. Because the oxygen is received from the ASU, exergy losses associated with oxygen separation have not been included.

3.3. Water to wet combustion chamber supply line with heat recovery

The water supply line to the WCC with heat recovery is extremely important because the temperature of the water supply affects the exergy losses in the combustion chamber. It is worth highlighting the data collected in Table 9 for the WCC pump ($P_{H2O\text{-}WCC}$) with work = 1.8 kW. Table 10 shows the most important information about the heat exchanger (HE1) with calculated heat duty = 48.6 kW.

3.4. Wet combustion chamber and expansion

First of all, it is necessary to distinguish Table 11, which contains the data of the WCC with chemical energy rate according to LHV = 282 kW and according to HHV = 317 kW. This is the table (Table 11) that captures the greatest amount of information, because in addition to the classical state parameters such as temperature, pressure, mass flow, it includes the exergy related both to physical parameters and the chemical energy carried in the fuel and the exergy degraded in the combustion process. It can be seen that inside the chamber there is a decrease in pressure of all flows up to 10 bar in accordance both with the flame, whether at the outlet of the chamber. Table 12 shows the results for the GT with an achievable work output = 90.4 kW. In addition, the GT^{bap} with work rate = 65.7 kW obtains a slightly lower work output (Table 13).

Table 8
Oxygen Compressor (C_{O2}), Work = 5.9 kW.

	RH, %				40	50	60	50	50
	X_{aCO_2}, ppm				375	375	375	417	1000
Function	Medium	t, °C	p, bar	$\dot{m}$, g/s	E^{tot}, kW				
Inlet	O_2	15	1.013	20.6	2.4	2.4	2.4	2.4	2.4
Outlet	O_2	313	10.5	20.6	7.9	7.9	7.9	7.9	7.9
	E_d, kW				0.4	0.4	0.4	0.4	0.4
	η_{ex}, %				94.7	94.7	94.7	94.7	94.7

Table 9
WCC pump ($P_{H2O\text{-}WCC}$), Work = 1.8 kW.

	RH, %				40	50	60	50	50
	X_{aCO_2}, ppm				375	375	375	417	1000
Function	Medium	t, °C	p, bar	$\dot{m}$, g/s	E^{tot}, kW				
Inlet	H_2O(liq)	33	1	62.9	7.8	5.9	4.4	5.9	5.9
Outlet	H_2O(liq)	35	225	62.9	9.2	7.4	5.8	7.4	7.4
	E_d, kW				0.4	0.4	0.4	0.4	0.4
	η_{ex}, %				96.3	95.4	94.3	95.4	95.4

Table 10
Heat Exchanger (HE1), Heat Duty = 48.6 kW.

		RH, %			40	50	60	50	50
		X_{aCO_2}, ppm			375	375	375	417	1000
Function	Medium	t, °C	p, bar	$\dot{m}$, g/s	E^{tot}, kW				
Inlet	H_2O(liq)	35	225	42.9	6.3	5.0	4.0	5.0	5.0
Outlet	H_2O(liq)	294	225	42.9	22.2	20.9	19.9	20.9	20.9
Inlet (exhaust)	H_2O(g), CO_2	323	0.078	100	41.9	39.7	37.8	39.5	38.4
Outlet (exhaust)	H_2O(g), CO_2	40	0.078	100	25.0	22.8	20.9	22.6	21.5
		E_d, kW			1.0	1.0	1.0	1.0	1.0
		η_{ex}, %			98.0	97.8	97.6	97.8	97.7

Table 11
Wet Combustion Chamber (WCC) with chemical energy rate according to LHV = 282.4 kW, and according to HHV = 316.9 kW.

		RH, %			40	50	60	50	50
		X_{aCO_2}, ppm			375	375	375	417	1000
Function	Medium	t, °C	p, bar	$\dot{m}$, g/s	E^{tot}, kW				
Inlet (syngas)	CO, CO_2, CH_4, C_3H_8, H_2	306	10.5	16.6	297.9	297.4	297.1	297.3	296.2
Inlet	O_2	313	10.5	20.6	7.9	7.9	7.9	7.9	7.9
Inlet	H_2O(liq)	181	225	20	5.8	5.2	4.7	5.2	5.2
Inlet	H_2O(liq)	294	225	42.9	22.2	20.9	19.9	20.9	20.9
Intermediary	O_2 (mixing with:), CO, CO_2, CH_4, C_3H_8, H_2	308	10.5	37.2	303.3	302.8	302.5	302.7	301.6
Flame	H_2O(g), CO_2	4260	10	37.2	271.1	270.7	270.4	270.6	269.5
Outlet	H_2O(g), CO_2	1100	10	100	207.3	205.0	203.1	204.9	203.7
		E_d, kW			126.5	126.5	126.5	126.5	126.5
		η_{ex}, %			62.1	61.8	61.6	61.8	61.7

Table 12
Gas Turbine (GT), Work = 90.4 kW.

		RH, %			40	50	60	50	50
		X_{aCO_2}, ppm			375	375	375	417	1000
Function	Medium	t, °C	p, bar	$\dot{m}$, g/s	E^{tot}, kW				
Inlet	H_2O(g), CO_2	1100	10	100	207.3	205.0	203.1	204.9	203.7
Outlet	H_2O(g), CO_2	672	1	100	112.5	110.2	108.3	110.0	108.9
		E_d, kW			4.5	4.5	4.5	4.5	4.5
		η_{ex}, %			97.8	97.8	97.8	97.8	97.8

Table 13
Gas Turbine below ambient pressure (GT^{bap}), Work = 65.7 kW.

		RH, %			40	50	60	50	50
		X_{aCO_2}, ppm			375	375	375	417	1000
Function	Medium	t, °C	p, bar	$\dot{m}$, g/s	E^{tot}, kW				
Inlet	H_2O(g), CO_2	672	1	100	112.5	110.2	108.3	110.0	108.9
Outlet	H_2O(g), CO_2	323	0.078	100	41.9	39.7	37.8	39.5	38.4
		E_d, kW			4.8	4.8	4.8	4.8	4.8
		η_{ex}, %			95.7	95.7	95.6	95.6	95.6

3.5. *Ending of the expansion with CO_2 processing*

Ending of the expansion with CO_2 processing can be found in Tables 14 and 15. SEC with separator is driven by a pump with required work = 18.2 kW. SEC set devices is characterized by a phase transformation together with an apparent destruction of exergy compared to the other devices (Table 14). It should be noted that a significant rate of exergy for the entire cycle is recycled between the inlet and outlet of the SEC precisely in the context of the results shown in Table 14. Table 15, on the other hand, collects data on the entire CO_2 capture process, namely: Carbon Capture Unit (CCU), HE3 and HE4 cooling heat duty = 12.3 kW, compressors $C_{CO2\text{-}1}$ and $C_{CO2\text{-}2}$ with work = 10.1 kW.

3.6. *nCO_2PP exergy efficiency*

While the cumulative efficiency of the power plant in the studied combination is 27.9 % [5], its exergy efficiency according to Eq. (8) is 33.3 % (base case) when related to the exergy of the sewage sludge used as input and is relatively constant for varying RH, although for the 1000 ppm CO_2 case (Fig. 3) this efficiency drops to 33.0 %, as can be seen in Fig. 3. Kang et al. [30] conducted an analysis of a cogeneration system with a gas turbine traditionally fueled by methane co-operating with a heat pump obtaining an exergetic efficiency of 22.6 %. The present value is lower than the nCO_2PP solution however, authors such as Yang et al. [31] and Samanta and Roy [32], through the implementation of a fuel cell, obtained excellent exergetic efficiencies, namely: 61.3 % and 47.5 %. The biomass-based integrated gasification combined cycle also has

Table 14
Spray Ejector Condenser (SEC) with Separator, Pump Work = 18.2 kW.

				RH, %	40	50	60	50	50
				X_{aCO_2}, ppm	375	375	375	417	1000
Function	Medium	*t*, °C	*p*, bar	$\dot{m}$, g/s	E^{tot}, kW				
Inlet (motive fluid)	H_2O(liq)	33	1	28,740	3564.3	2712.1	2015.8	2712.1	2712.1
Inlet (exhaust)	H_2O(g), CO_2	40	0.078	100	25.0	22.8	20.9	22.6	21.5
Outlet	H_2O(g), CO_2	35	1	23.7	10.0	10.0	10.0	9.8	8.7
Outlet	H_2O(liq)	35	1	28,816	3586.2	2731.8	2033.6	2731.8	2731.8
				E_d, kW	11.3	11.3	11.3	11.3	11.3
				η_{ex}, %	99.7	99.6	99.5	99.6	99.6

Table 15
Carbon Capture and Utilization (CCU), HE3 and HE4 cooling heat duty = 12.3 kW, compressors $C_{CO2\text{-}1}$ and $C_{CO2\text{-}2}$ Work = 10.1 kW.

				RH, %	40	50	60	50	50
				X_{aCO_2}, ppm	375	375	375	417	1000
Function	Medium	*t*, °C	*p*, bar	$\dot{m}$, g/s	E^{tot}, kW				
Inlet	H_2O(g), CO_2	35	1	23.7	10.0	10.0	10.0	9.8	8.7
Outlet	H_2O(liq)	65	80	0.5	0.07	0.06	0.05	0.06	0.06
Outlet	H_2O(g), CO_2	65	80	23.2	15.0	15.0	15.0	14.8	13.7
Inlet (waste heat water)	H_2O(liq)	35	225	20	2.9	2.3	1.9	2.3	2.3
Outlet (waste heat water)	H_2O(liq)	181	225	20	5.8	5.2	4.7	5.2	5.2
				E_d, kW	2.2	2.2	2.2	2.2	2.2
				η_{ex}, %	90.6	90.4	90.1	90.3	89.8

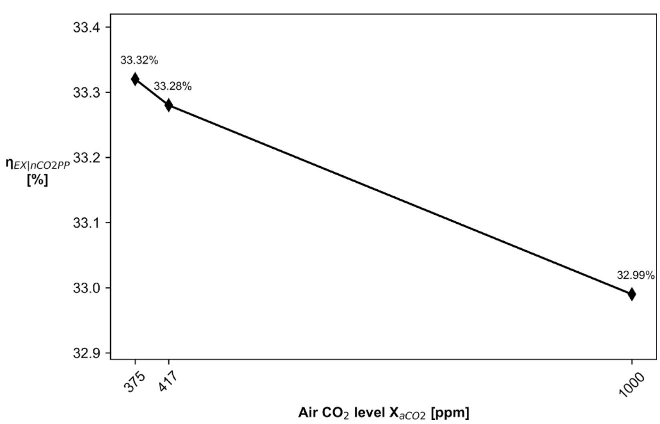

Fig. 3. nCO_2PP exergy efficiency in changing air CO_2 concentrations.

similar positive effects on the final efficiency as nCO_2PP. BECCS based on BIGCC with pre-combustion CO_2 capture, fueled by sawdust, allows achieving exergetic efficiencies of 38.8 % [35]. On the other hand, Ghiat et al. [33] demonstrated that BECCS based on BIGCC fueled by date pits achieves an exergetic efficiency of 57.2 %. The highest exergetic efficiencies have been reported in the work of Ebrahimi and Ziabasharhagh [34], who analyzed an innovative solution with a wide range of devices, namely: BECCS based on BIGCC with pre-combustion CO_2 capture, electricity, heat and LNG production fueled by rice husk. They presented the exergy efficiency of 74.1 % which is made possible by the hierarchical temperature distribution used throughout the system [34]. However, none of the present works included the ejector in the set of working equipment, which was subjected to exergetic analysis in the work of Ertesvåg et al. [6]. For a more detailed discussion of the effect of the ejector on the exergetic efficiency of the entire system when used as an SEC, see the following subsection.

3.7. SEC influence on nCO_2PP exergy efficiency

From Ertesvåg et al. [6] it is known that increasing the pressure of the flue gas entering the SEC (at the outlet of the last gas turbine) in the range of 0.068–0.1 bar increases the SEC exergy destruction and reduces the turbine power and cycle efficiency, without much effect on the other units. In addition, [6] found that increasing the temperature range of the same flow from 32 to 120 °C had similar effects. However, work by other authors suggests that the result is not so clear-cut. Mikielewicz et al. [10] clearly show analytically and experimentally that the SEC characteristics are not linear. And the optimal operating conditions taking into account the interactions, water droplets, volume fraction of CO_2 in the exhaust gas mixture along with the significant pressure influence prevailing in different parts of the SEC change and we should not overlook this. Subsequently, the studies of Madejski et al. [9] and Kuś and Madejski [71] also show a wealth of phenomena and a wide range of parameters affecting SEC performance. In addition, Stasiak et al. [72] performed an analysis of the nCO_2PP cycle with oRc and showed that temperature and condensation pressure also have a large effect on complex cycles. This trend was confirmed for five media, together with a special analysis of the temperature distribution in the condenser and regenerative exchanger part (HE1). These results led the authors to extend the model in this paper from the article by Ertesvåg et al. [6] to include effects related to the mutual influence of the regenerative exchanger on the SEC. This includes parameters such as the condensing temperature of the steam or the power demand of the SEC pumps and the power output of the turbines. Assuming a constant volumetric entrainment ratio of 6, together with the change in CO_2 in the flue gas, the above optimum and operating conditions must be re-evaluated.

On the one hand, the power decrease of the GT^{bap} turbine is almost linear (Fig. 4). On the other hand, the decrease of the power consumed by the SEC pumps is parabolic, which consequently determines the optimal operation of the whole nCO_2PP cycle. The inverted parabola of the nCO_2PP exergetic efficiency reaches the maximum value of 33.6 % at a pressure of $P_4 = P_5 = 0.11$ bar, which corresponds to the beginning of the condensation of steam in binary mixture with CO_2 at a temperature of 45 °C and is maintained at point 5 before the SEC. Fig. 5. shows the change in the molar fraction of CO_2 (X_5) at the SEC inlet. This is closely related to the heat recovery of the HE1 regenerative heat exchanger. As the temperature of the 1^{H2O} water increases after regeneration, we can feed less fuel to the WCC and thus the amount of carbon dioxide in the flue gas decreases. However, the amount of CO_2 is also related to the CO_2 capture capability and the amount of compressed refrigerant in the CCU. For the molar fraction upstream of the CCU system ($X_{1\text{-}CCU}$), the

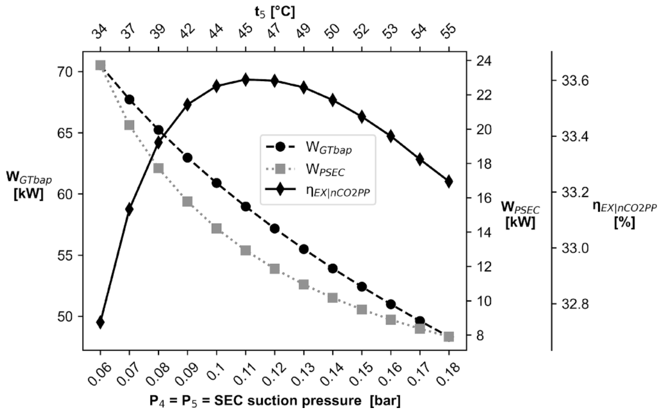

Fig. 4. SEC suction pressure sensitivity analysis on GT^{bap} power production (W_{GT} ^{bap}), SEC pump power consumption (W_{PSEC}), and nCO_2PP cycle exergetic efficiency ($\eta_{ex|nCO_2PP}$).

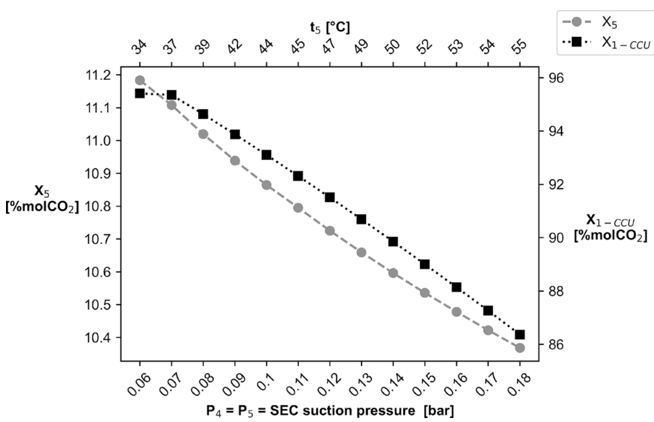

Fig. 5. SEC suction pressure sensitivity analysis on CO_2 mole fraction (X_5) and CO_2 mole fraction after capture ($X_{1\text{-}CCU}$) before CCU.

characteristics of carbon dioxide change its nature and at 0.07 bar there is a decrease in the molar fraction of CO_2. At 0.06 and 0.07 bar, there is only residual water vapor due to the partial pressure of water in the gas mixture, which prevents all the water vapor from condensing at a given temperature and pressure. However, at higher temperatures, the concentration of CO_2 directed to the CCU compressor decreases, below 95 %, which means that the proportion of post-separation steam increases for these assumptions of SEC operation (volumetric entrainment ratio = 6, related to CO_2 volume). The present result has its correlation with the obtained exergy for SEC in Fig. 5. It is worth noting that GT^{bap} and CCU are adjacent units in line with SEC, so Fig. 6 shows the change in

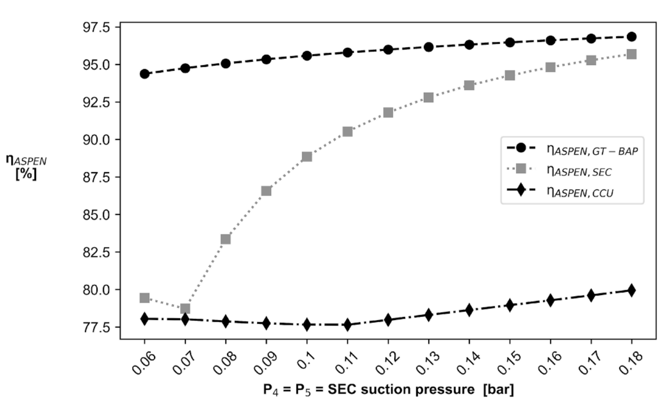

Fig. 6. SEC suction pressure sensitivity analysis on GT^{bap} , SEC and CCU unit exergy efficiency based on Aspen exergy.

exergetic efficiency (based on Aspen exergy) of these units. Only the turbine efficiency does not follow the changing trend, as the exergetic efficiency of the CCU starts to increase again at a pressure value of 0.11 bar.

3.8. Sewage sludge composition influence on nCO_2PP exergy efficiency

Dry organic composition (C, H, O, N, S) of sewage sludge from 17 experimental [54,56–70] and 83 simulated cases are stacked on scatter plots in Fig. 7, for a total of 100 compositions. To show the agreement of these results, Table 16 shows the statistical comparison between the simulated and experimental elemental compositions (C, H, O, N, S) of the p-values, mean, minimum and maximum. The p-values indicate whether the distributions are significantly different from a normal distribution under null hypothesis testing [55]. Typically, a p-value threshold of 0.05 is used to determine statistical significance, although this is not binding and may vary depending on the context of the study. In other words, the p-value represents the probability of obtaining results as extreme as those observed if the distribution were normal. Here, the p-value for the element sulfur is less than 0.05, which appears to be a statistically significant value, since some of the experimentally obtained sludge contents of this element are reported to be 0 %, which is unlikely in real conditions, but in the simulated compositions it can be seen that sulfur, as well as other elements, are in good statistical agreement with the input.

Ten selected dry and purified syngas compositions obtained after scrubbing and subsequent compression and fed to the combustor are shown in Fig. 8. This Fig. shows five selected syngas compositions calculated from experimentally derived sewage sludge on the left and five from the Monte Carlo simulation in this study on the right. It is worth noting that there is no C_3H_8 component in the results, as in the base case, because the Gibbs reactor principle, by minimizing the Gibbs energy, does not yield this component in significant amounts. In the context of the results obtained, it is worth mentioning that in Fig. 8 there is a trend corresponding to the production of hydrogen in the highest proportion, however, the second component in the results presented is CO_2. This is due to the fact that the chemical equilibrium in the water–gas shift reaction has shifted towards the production of CO_2 and H_2. This is related to the specific composition of sewage sludge, and unlike the results presented by Zheng et al. [73] for municipal solid waste, the contribution of CO is much lower than that of CO_2.

To show how the different compositions (100 compositions) affect various parameters of the power plant, Figs. 9-13 show the percentile bars of the calculated LHV of the sewage sludge (Fig. 9), the exergetic efficiency $\eta_{ex\,WCC}$ of the WCC (Fig. 10), the exergetic efficiency $\eta_{aspen\,SEC}$ (based on Aspen exergy) of the SEC (Fig. 11) and the exergetic efficiency $\eta_{ex|nCO_2PP}$ of the nCO_2PP power plant (Fig. 12), the CO_2 mole fraction $X_{WCC\,exh.\,CO_2}$ in the WCC flue gas (Fig. 13). These percentile bars show the 0th percentile as “Min”, the 25th percentile as “Q1”, the 50th percentile as “Median”, the 75th percentile as “Q3”, the 100th percentile as “Max” and the mean as a black dot.

Fig. 9 shows the calculated LHV of sewage sludge with ash and moisture which, despite significant differences between the median and maximum values, shows the range of feedstocks supplied for syngas production. The LHV range of sewage sludge is approximately between 9.5 and 20 MJ/kg, which is comparable to the range of 11 to 20 MJ/kg from [53]. Both the median and the mean remain above 14400 kJ/kg, which is sufficient to produce a fuel with a significant volume fraction of hydrogen. The presented feedstock with compositions as shown in Fig. 7 and with LHV values in the ranges shown in Fig. 9 was gasified in a Gibbs reactor. It is worth noting that the exergetic efficiency of the WCC shown in Fig. 10 is within a much narrower range (62.3 to 64.5 %) than the LHV. In addition, the exergetic efficiency of the SEC, shown in Fig. 11, does not change significantly (89.4 to 90.5 %) when the fuel is changed. Taking into account these two key devices and their relatively small

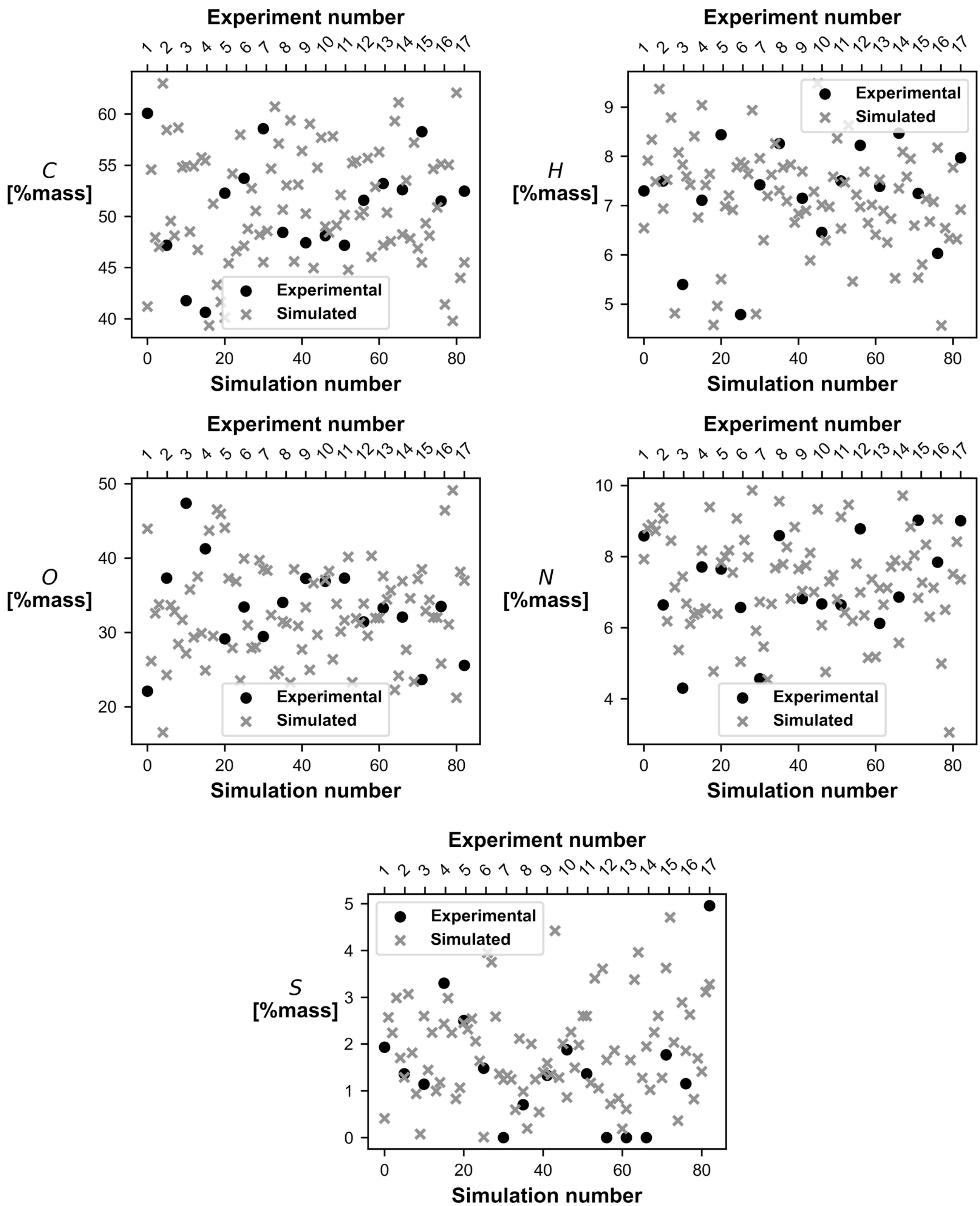

Fig. 7. Scatter plots showing the elemental composition (C, H, O, N, S) of dry organic sludge from experimental data and the result of Monte Carlo simulations.

changes in exergetic efficiency, it should be noted that the wide range (33.6 to 39.7 %) of the exergetic efficiency (Fig. 12) of the whole nCO_2PP cycle is related to the fuel exergy and is partly associated with a significant change in the CO_2 content (11 to 17 %) of the mixture at the outlet of the WCC (Fig. 13), which becomes the product of the CCU at the end. In addition, it should be noted that, as demonstrated by the analysis of Baratieri et al. [74], the biomass syngas produced can be used in internal combustion engines and combined cycle gas turbines (CCGT), as an alternative to the nCO_2PP system presented. However, in their case the LHV was about 16 MJ/kg, which is also within the range of the results in Fig. 9. The CCGT system is worthy of comparison in that the calculations of Baratieri et al. included a similar temperature value of

Table 16
Summary of multivariate Monte Carlo simulation results for sewage sludge components in mass fractions.

Element	Experimental				Simulation			
	p-value, –	mean, %	min, %	max, %	p-value, –	mean, %	min, %	max, %
C	0.526	50.9	40.6	60.1	0.325	51.1	39.3	63.0
O	0.810	33.2	22.1	47.4	0.626	32.5	16.6	49.1
N	0.138	7.2	4.3	9.0	0.303	7.3	3.1	9.9
S	0.033	1.5	0.0	5.0	0.104	1.9	0.0	4.7
H	0.070	7.2	4.8	8.5	0.084	7.1	4.6	9.5

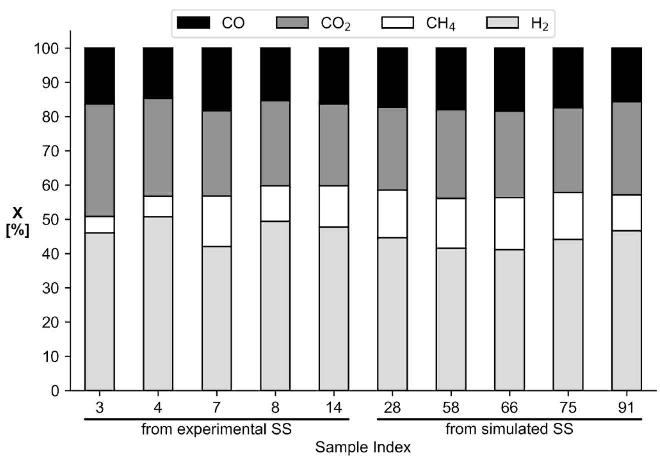

Fig. 8. Selected molar compositions of CO, CO_2 , CH_4 , and H_2 of the syngases fed to the WCC (comparison of data obtained from the experimental sludge and simulated by the Monte Carlo method).

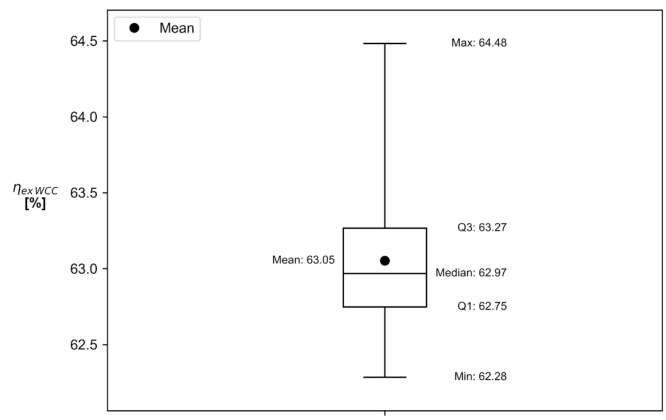

Fig. 10. Exergetic efficiency of WCC after simulations with 100 different sewage sludge compositions.

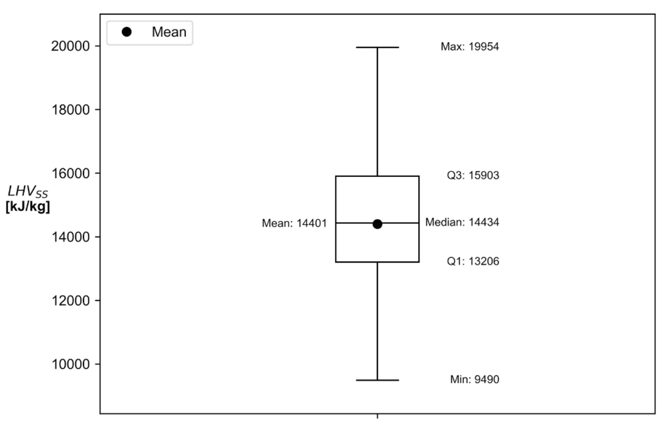

Fig. 9. Lower heating value of sewage sludge including ash and moisture for 100 sewage sludge compositions.

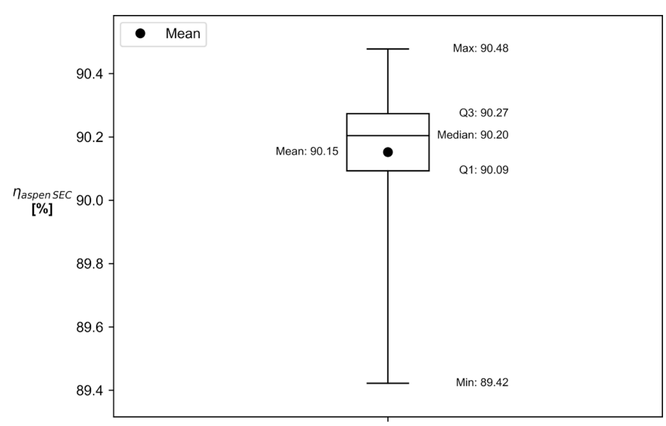

Fig. 11. Exergetic efficiency of SEC after simulations with 100 different sewage sludge compositions.

the exhaust gas from the combustion chamber, namely 1187 °C.

With the sample of 100 simulation results, correlations of selected variables with nCO_2PP exergy efficiency can be extracted, as shown in Fig. 14. Each correlation shows the strength of the relationship between changing variables (selected variable and nCO_2PP exergy efficiency) due to different sewage sludge compositions. The value of the correlation can be positive or negative, with a maximum of 1 or −1. Correlations above 0.7 or below −0.7 can be considered as strong correlations, while correlations below 0.5 can be considered as weak correlations that can be ignored. It is important to note that these correlations refer to the given sludge compositions under the conditions of this study, i.e. the sludge is never pure carbon and the resulting syngas is never pure CH_4 or H_2, but a mixture of CO, CO_2, CH_4 and H_2 as shown in Table 16 and Figs. 7 and 8.

The carbon element in the sewage sludge composition has the strongest relationship with the nCO_2PP exergy efficiency with a correlation of 0.93, while the oxygen element has the strongest negative correlation of −0.82. Higher oxygen content in the sewage sludge (correlation −0.82) leads to higher CO_2 in the syngas (correlation −0.67), which increases the CO_2 content in the WCC flue gas (correlation −0.61). However, the hydrogen element has a weak correlation of 0.37 and this correlation could be ignored. The LHV of the sewage sludge, which is also highly related to three of these elements, has a correlation of 0.85 with the nCO_2PP exergy efficiency. While increasing the LHV of the sewage sludge means increasing the exergy of a fuel, which increases the denominator of the nCO_2PP exergy efficiency in Eq. (8), it actually decreases this denominator by decreasing the sewage sludge mass flow requirement in the gasification process, resulting in a higher LHV of the syngas, and with this decrease in sewage sludge mass flow, the bleed flow before the second turbine GT^{bap} also decreases

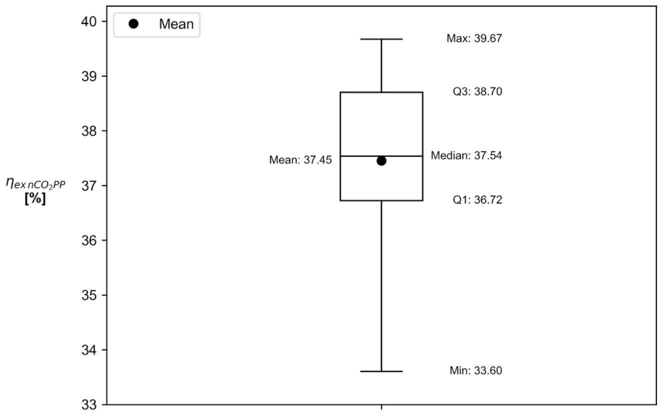

Fig. 12. Exergetic efficiency of nCO_2PP cycle after simulations with 100 different sewage sludge compositions.

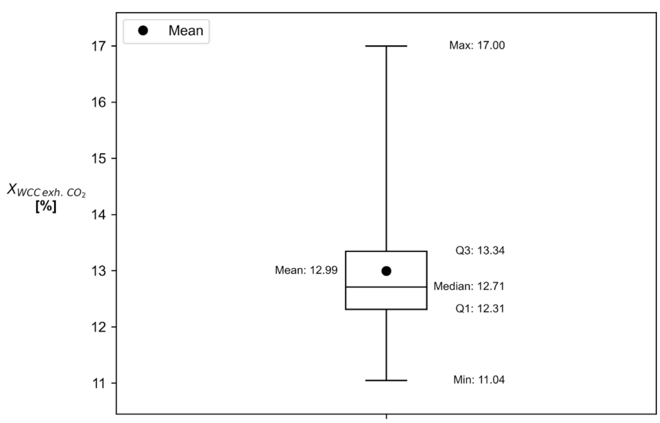

Fig. 13. WCC exhaust CO_2 mole fraction after simulations with 100 different sewage sludge compositions.

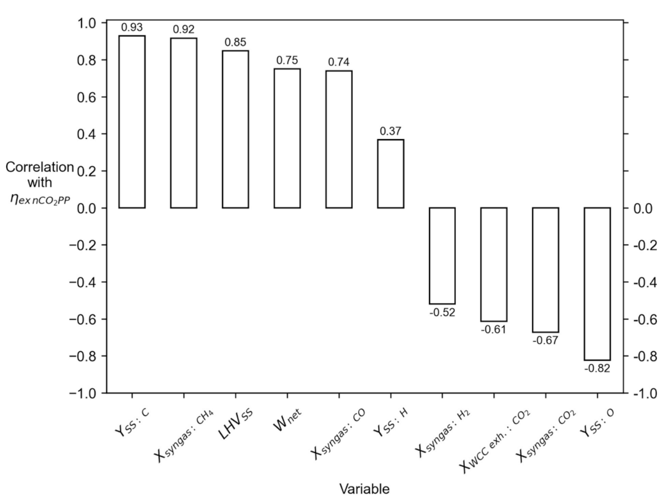

Fig. 14. Correlation of selected variables with the exergetic efficiency of the nCO_2PP cycle.

(which is kept constant as 0.846 fraction of the sewage sludge mass flow requirement in this study). All this while maintaining 1100 °C and 100 g/s in the WCC exhaust.

The net power output of the power plant is positively correlated (0.75) with the nCO_2PP exergy efficiency, which is the expected result while being in the counter of Eq. (8).

The CH_4 in the syngas correlation of 0.92 is the second strongest after the C element. Although it seems to be related to the correlation of the C element with the exergy efficiency, it also seems that either it should follow the correlation of H_2 or vice versa due to the possession of four hydrogen atoms in the methane structure, but H_2 in the syngas is negatively correlated with the nCO_2PP exergy efficiency with a value of −0.52. The CO component shares this place with a correlation of 0.74. This relationship, where CH_4 and CO have a positive correlation and H_2 a negative one on the nCO_2PP efficiency, is related to the fact that the density of the combustible gases is also important (CH_4 has a much higher LHV in volume than H_2), which means that a higher H_2 gas content means higher compressor power consumption due to its low density, negating its benefit in reducing CO_2 in the WCC flue gas. While CO has only a slightly higher LHV in volume terms than H_2, its positive correlation with nCO_2PP exergy efficiency could be related to the water–gas reaction in the gasifier, where having more CO and H_2O (which is condensed in the syngas treatment) is offset by having less CO_2 and H_2, both of which have negative correlations.

However, with carbon element in gas components such as CH_4 or CO (correlation 0.74), there is also a change in the CO_2/H_2O fraction in the flue gas. Here, higher CO_2 content (correlation −0.61) in the WCC exhaust gas leads to higher SEC pump power consumption due to higher water mass flow as motive fluid requirement due to constant volume entrainment ratio related to CO_2 volume, reducing net power output and exergetic efficiency. However, it is important to note that although the CO_2 in the WCC exhaust gas (correlation −0.61) is also derived from carbon fuels such as CH_4 and CO in the syngas, the fraction of CO_2 in the WCC exhaust gas usually decreases with higher CH_4 supply, as higher LHV syngas requires more H_2O injection to maintain the temperature of 1100 °C in the WCC. Thus, the highest correlation of CH_4 among all syngas components with nCO_2PP exergy efficiency is related to the fact that CH_4 has a much higher density than H_2, and part of its advantage over CO is due to its much higher LHV and the absence of the oxygen element.

As mentioned above, these correlations are only valid for the studied sewage sludge compositions in this power plant design with complex loop system. It would be different under different conditions, e.g. if much broader sewage sludge compositions were used or different gasifier conditions were simulated, i.e. pure CO gas as WCC fuel (correlation with nCO_2PP efficiency = 0.74) would most likely no longer be positively correlated with the power plant exergy efficiency due to the high CO_2 fraction resulting in WCC exhaust, which would be reflected in higher SEC pump power consumption.

3.9. Overall discussion and recommendations

There are three major challenges that arise in the proposed system. The first challenge is to replace gasification with steam or a mixture of steam and CO_2 with gasification using a plasmotron [75]. As preliminary studies show, the use of electricity to sustain the electrode arc in a plasmotron is at the limit of energy efficiency, so converter gasification is closer to implementation. The second major challenge in the implementation of the present system is the efficient cooling of the walls of the wet combustion chamber [7]. Both experimental and numerical studies have failed to confirm exactly how and how much water should be injected to achieve both the required material temperature limits and to ensure complete evaporation of the coolant. The third fundamental challenge is to reduce the amount of water that drives the SEC [9], so that the efficient separation of water from CO_2 can follow [76]. Thus, the overall challenge is the lack of maturity of the nCO_2PP technology and the need for further experimental research. A significant limitation is that even if the technologies reach maturity, the sludge resource will still be a small fraction of the total electricity production. Hence, in general, there are technological barriers related to refinement of the parameters and implementation of equipment operation. Therefore, further research and implementation studies related to a dedicated system design adapted to the sewage sludge resources of an average wastewater treatment plant are planned in the future. In addition, further research could be aimed at changing the configuration of the system, such as replacing the SEC-type condenser with a dedicated heat exchanger. Another alternative is to move away from low-calorie fuel and adapt the nCO_2PP unit to fuels based on hydrogen technologies, such as pure hydrogen or methanol from environmentally friendly sources. It is important to note that due to the wide range of sewage sludge compositions, the syngas composition produced in reality depending on the applied technology would be different from the Gibbs reactor output in this simulation, but to correctly predict the syngas results, a complex reactor model would need to be prepared based on experiment on a wide range of used sewage sludge compositions to prove its use, so the Gibbs reactor, which is fundamentally an ideal conditions reactor, was used. Therefore, it is important to emphasize that this approach allows modeling the effect of sewage sludge composition variability on power plant parameters, as opposed to single deterministic scenarios.

Furthermore, an important and current research direction is to use experimental results to create numerical models supported by artificial intelligence to analyze system behavior in real time in the context of diagnostics and optimization of nCO_2PP operation. This approach will allow significant improvements in the context of environmental, energy and exergy parameters.

4. Conclusions and perspectives

Second law analysis has been conducted on nCO_2PP. The analyses gave an insight into the integrated system of the gasifier and the nCO_2PP cycle, taking into account the influence of the relative humidity and the CO_2 content in the air, which is translated into the chemical exergy of the components in relation to the dead state. The conducted analyses showed that the lowest exergy efficiency is characterized by a wet combustion chamber with a value of about 62 %. However, exergy losses affecting the efficiency of this device are unavoidable. Another device with a relatively low exergy efficiency is the gasifier unit and the heat exchanger of the gas scrubber with efficiencies of 89 % and 87 %, respectively. Also, in this set of devices, the possibilities to reduce the exergy destruction are limited. The exergy efficiency of the power plant was found to be 33.3 % for the base case. Significant prospects for reducing exergy destruction are offered by the heat exchanger of the gas scrubber because the waste heat from this device can be used to drive organic Rankine cycles or to produce oxygen in oxygen transport membranes.

This study also showed that the plant can be optimized in terms of efficiency depending on the conditions. The optimal operating parameters of the SEC were sought and found to be 0.11 bar suction pressure for the GT^{bap} turbine vacuum in the base case, which increased the exergetic efficiency to 33.6 %. Furthermore, the exergetic efficiency of the power plant obtained from different sewage sludge compositions on the power plant analysis ranged from 33.6 to 39.7 %. Here, the analysis was performed using a Gibbs reactor, with a portion of the scrubber waste heat diverted to the gasification reactor, and turbine bleed stream as the gasification agent, while the base case was based on real results using steam gasification from other authors' work. Furthermore, the main novelty of this work in terms of Monte Carlo simulations of sewage sludge composition is the attempt, for the first time in the literature, to standardize the range of sewage sludge compositions for one's own purposes by generating data using reference experimental data from the literature. These results are relevant for process design and optimization, especially when it is not possible to use a deterministic approach by assuming an arbitrary composition of the syngas mixture fed to the combustor or the sewage sludge composition fed to the gasifier. The conclusions of the BECCS power plant exergy analysis are as follows:

- The combination of higher carbon (C) and lower oxygen (O) content in the sewage sludge compositions leads to higher nCO_2PP exergy efficiency.
- Higher LHV syngas translates into lower CO_2 concentration in the WCC exhaust, as more H_2O injection is required to maintain the temperature of 1100 °C in the WCC exhaust.
- The syngas is most beneficial in terms of nCO_2PP power plant exergy efficiency when it is over-represented with CH_4, as it combines the advantages of carbon and H_2, both having high LHV, while maintaining low density due to the "compact" molecular structure of methane compared to pure H_2.
- CO_2, either in the syngas or in the WCC flue gas, reduces the nCO_2PP exergy efficiency due to the increased power consumption of the SEC pump, which pumps motive fluid water in an amount related to the CO_2 volume.
- The power plant exergy efficiency shows a significant dependence on the sewage sludge composition and LHV.

As a perspective solution, the results with various sewage sludge compositions can be applied to feed a machine learning model such as a neural network using the results presented in this study, instead of solving a complex first-principles model (based on fundamental physical and chemical laws) as in this study.

Declaration of competing interest

The authors declare that they have no known competing financial interests or personal relationships that could have appeared to influence the work reported in this paper.

Acknowledgments

The research leading to these results has been funded by the Norway Grants 2014-2021 via the National Centre for Research and Development. This article has been prepared within the project "Negative CO_2 Emission Gas Power Plant" — NOR/POLNORCCS/NEGATIVE-CO2-PP/0009/2019-00, which is co-funded by the "Applied Research" program under the Norwegian Financial Mechanism 2014-2021 POLNOR CCS 2019 for the development of CO_2 capture solutions integrated in power and industrial processes. Part of the work is a result of a project realized by Paweł Ziółkowski and financial support of these studies from Gdańsk University of Technology by No. 2/1/2022/IDUB/IV.2a/Eu grant under the Europium Short-Term Outgoing Visits program is gratefully acknowledged. The author, Kamil Stasiak, acknowledges the financial support of the PROM program funded by the Polish National Agency for Academic Exchange (NAWA) (agreement number PPI/PRO/2019/1/00009/U/00001), which facilitated a research visit to the Norwegian University of Science and Technology (NTNU) and enabled the study of exergy analysis.

Appendix A. Supplementary data

Supplementary data to this article can be found online at https://doi.org/10.1016/j.applthermaleng.2024.125312.

Data availability

Data will be made available on request.

References

[1] Negative CO2 Emission Gas Power Plant Project site, (2023). nco2pp.com (accessed January 4, 2024).

[2] P. Ziółkowski, J. Badur, H. Pawlak- Kruczek, K. Stasiak, M. Amiri, L. Niedzwiecki, K. Krochmalny, J. Mularski, P. Madejski, D. Mikielewicz, Mathematical modelling of gasification process of sewage sludge in reactor of negative CO2 emission power plant, Energy 244 (2022) 122601, https://doi.org/10.1016/j.energy.2021.122601.

[3] P. Ziółkowski, P. Madejski, M. Amiri, T. Kuś, K. Stasiak, N. Subramanian, H. Pawlak-Kruczek, J. Badur, Ł. Niedźwiecki, D. Mikielewicz, Thermodynamic analysis of negative CO2 emission power plant using aspen plus, aspen Hysys, and ebsilon software, Energies (basel) 14 (2021), https://doi.org/10.3390/en14196304.
[4] K. Stasiak, P. Ziółkowski, D. Mikielewicz, Carbon Dioxide Recovery Skid, Progress in Petrochemical, Science 3 (2020) 362–364. https://doi.org/10.31031/pps.2020.03.000570.
[5] P. Ziółkowski, K. Stasiak, M. Amiri, D. Mikielewicz, Negative carbon dioxide gas power plant integrated with gasification of sewage sludge, Energy 262 (2023), https://doi.org/10.1016/j.energy.2022.125496.
[6] I.S. Ertesvåg, P. Madejski, P. Ziółkowski, D. Mikielewicz, Exergy analysis of a negative CO2 emission gas power plant based on water oxy-combustion of syngas from sewage sludge gasification and CCS, Energy 278 (2023) 127690, https://doi.org/10.1016/J.ENERGY.2023.127690.
[7] P. Ziółkowski, K. Stasiak, M. Ditaranto, S. Wiseman, D. Mikielewicz, Negative CO2 Emission Gas Power Plant As Technology for Utilization of Sewage Sludge, Production of Electrical Energy, and CO2 Capture - Case of Chamber Under Transpiration Cooling, in: Volume 5: Cycle Innovations, American Society of Mechanical Engineers, 2024. https://doi.org/10.1115/GT2024-128805.
[8] M. Froissart, T. Ochrymiuk, Novel wet combustion chamber concept CFD studies with triple water inlet, Energy 278 (2023) 127854, https://doi.org/10.1016/J.ENERGY.2023.127854.
[9] P. Madejski, K. Banasiak, P. Ziółkowski, D. Mikielewicz, J. Mikielewicz, T. Kuś, M. Karch, P. Michalak, M. Amiri, P. Dąbrowski, K. Stasiak, N. Subramanian, T. Ochrymiuk, Development of a spray-ejector condenser for the use in a negative CO2 emission gas power plant, Energy 283 (2023) 129163, https://doi.org/10.1016/J.ENERGY.2023.129163.
[10] D. Mikielewicz, M. Amiri, M. Klugmann, J. Mikielewicz, A novel concept of enhanced direct-contact condensation of vapour- inert gas mixture in a spray ejector condenser, Int J Heat Mass Transf 216 (2023) 124576, https://doi.org/10.1016/J.IJHEATMASSTRANSFER.2023.124576.
[11] M. Kaszuba, P. Ziółkowski, D. Mikielewicz, Performance of cryogenic oxygen production unit with exhaust gas bleed for sewage sludge gasification and different oxygen purities, Archives of Thermodynamics (2023). https://doi.org/10.24425/ATHER.2023.147537.
[12] P. Ziółkowski, Ł. Witanowski, P. Klonowicz, D. Mikielewicz, High-speed multi-stage gas-steam turbine with flow bleeding in a novel thermodynamic cycle for decarbonizing power generation, Renew Energy 237 (2024) 121655, https://doi.org/10.1016/J.RENENE.2024.121655.
[13] I.S. Ertesvåg, Sensitivity of chemical exergy for atmospheric gases and gaseous fuels to variations in ambient conditions, Energy Convers Manag 48 (2007) 1983–1995, https://doi.org/10.1016/J.ENCONMAN.2007.01.005.
[14] J. Szargut, Chemical exergies of the elements, Appl Energy 32 (1989) 269–286, https://doi.org/10.1016/0306-2619(89)90016-0.
[15] M. Aghbashlo, M. Tabatabaei, M.H. Nadian, S. Soltanian, H. Ghasemkhani, A. Shafizadeh, S.S. Lam, Determining biomass chemical exergy using a novel hybrid intelligent approach to promote biomass-based biorefineries, J Clean Prod 277 (2020) 124089, https://doi.org/10.1016/J.JCLEPRO.2020.124089.
[16] H. Qian, W. Zhu, S. Fan, C. Liu, X. Lu, Z. Wang, D. Huang, W. Chen, Prediction models for chemical exergy of biomass on dry basis from ultimate analysis using available electron concepts, Energy 131 (2017) 251–258, https://doi.org/10.1016/J.ENERGY.2017.05.037.
[17] F. Zhang, S. Wang, Y. Li, W. Chen, L. Qian, Thermodynamic analysis of a supercritical water gasification – oxidation combined system for sewage sludge treatment with cool wall reactor, Energy Convers Manag 247 (2021) 114708, https://doi.org/10.1016/J.ENCONMAN.2021.114708.
[18] P.M. Ruya, R. Purwadi, S.S. Lim, Supercritical water gasification of sewage sludge for power generation– thermodynamic study on auto-thermal operation using Aspen Plus, Energy Convers Manag 206 (2020) 112458, https://doi.org/10.1016/J.ENCONMAN.2019.112458.
[19] T. Sung, S. Kim, K.C. Kim, Thermoeconomic analysis of a biogas-fueled micro-gas turbine with a bottoming organic Rankine cycle for a sewage sludge and food waste treatment plant in the Republic of Korea, Appl Therm Eng 127 (2017), https://doi.org/10.1016/j.applthermaleng.2017.08.106.
[20] J.Y. Kang, D.W. Kang, T.S. Kim, K.B. Hur, Economic evaluation of biogas and natural gas co-firing in gas turbine combined heat and power systems, Appl Therm Eng 70 (2014) 723–731, https://doi.org/10.1016/J.APPLTHERMALENG.2014.05.085.
[21] H. Nikpey Somehsaraei, M. Mansouri Majoumerd, P. Breuhaus, M. Assadi, Performance analysis of a biogas-fueled micro gas turbine using a validated thermodynamic model, Appl Therm Eng 66 (2014) 181–190, https://doi.org/10.1016/J.APPLTHERMALENG.2014.02.010.
[22] A. Abuşoğlu, E. Özahi, A.İ. Kutlar, S. Demir, Exergy analyses of green hydrogen production methods from biogas-based electricity and sewage sludge, Int J Hydrogen Energy 42 (2017) 10986–10996, https://doi.org/10.1016/J.IJHYDENE.2017.02.144.
[23] K.J. Ptasinski, C. Hamelinck, P.J.A.M. Kerkhof, Exergy analysis of methanol from the sewage sludge process, Energy Convers Manag 43 (2002) 1445–1457, https://doi.org/10.1016/S0196-8904(02)00027-4.
[24] L. Szablowski, P. Krawczyk, K. Badyda, S. Karellas, E. Kakaras, W. Bujalski, Energy and exergy analysis of adiabatic compressed air energy storage system, Energy 138 (2017), https://doi.org/10.1016/j.energy.2017.07.055.
[25] P. Krawczyk, Ł. Szabłowski, S. Karellas, E. Kakaras, K. Badyda, Comparative thermodynamic analysis of compressed air and liquid air energy storage systems, Energy 142 (2018) 46–54, https://doi.org/10.1016/J.ENERGY.2017.07.078.
[26] W. Chan, T. Morosuk, X. Li, H. Li, Exergoeconomic Analysis and Tri-Objective Optimization of the Allam Cycle Co-Fired by Biomass and Natural Gas, Journal of Energy Resources Technology, Transactions of the ASME 145 (2023), https://doi.org/10.1115/1.4062528.
[27] J. García-Domínguez, A.M. Blanco-Marigorta, J. Daniel Marcos, Analysis of a solar driven ORC-absorption based CCHP system from a novel exergy approach, Energy Convers. Manage.: X 19 (2023) 100402, https://doi.org/10.1016/J.ECMX.2023.100402.
[28] C. Fu, T. Gundersen, Using exergy analysis to reduce power consumption in air separation units for oxy-combustion processes, Energy 44 (2012) 60–68, https://doi.org/10.1016/J.ENERGY.2012.01.065.
[29] J. Szargut, Exergy method: technical and ecological applications, International Series on Developments in Heat Transfer 18 (2005).
[30] S. Kang, H. Li, L. Liu, J. Lei, G. Zhang, Exergy analysis of a novel CHP-GSHP coupling system, Appl Therm Eng 93 (2016) 308–314, https://doi.org/10.1016/j.applthermaleng.2015.09.039.
[31] S. Yang, A. Liang, S. Peng, Z. Liu, C. Deng, N. Xie, Energy, exergy and exergo-economic analysis of a novel HT-PEMFC based cogeneration system integrated with plasma gasification of food waste, Appl Therm Eng 246 (2024), https://doi.org/10.1016/j.applthermaleng.2024.122924.
[32] S. Samanta, D. Roy, Molten carbonate fuel cell integrated hybrid system for clean and efficient power generation, Appl Therm Eng 226 (2023), https://doi.org/10.1016/j.applthermaleng.2023.120294.
[33] I. Ghiat, A. AlNouss, G. McKay, T. Al-Ansari, Biomass-based integrated gasification combined cycle with post-combustion CO2 recovery by potassium carbonate: Techno-economic and environmental analysis, Comput Chem Eng 135 (2020), https://doi.org/10.1016/j.compchemeng.2020.106758.
[34] A. Ebrahimi, M. Ziabasharhagh, Energy and exergy analyses of a novel integrated process configuration for tri-generation heat, power and liquefied natural gas based on biomass gasification, Energy Convers Manag 209 (2020), https://doi.org/10.1016/j.enconman.2020.112624.
[35] L. Han, J. Zhao, N. Rong, Z. Wang, Z. Qi, Z. Shen, H. Ding, H. Yu, Energy and exergy analyses of biomass IGCC power plant using calcium looping gasification with in situ CO2 capture and negative carbon emission, Biomass Convers Biorefin (2023), https://doi.org/10.1007/s13399-023-04357-9.
[36] Y. Xiang, L. Cai, Y. Guan, W. Liu, T. He, J. Li, Study on the biomass-based integrated gasification combined cycle with negative CO2 emissions under different temperatures and pressures, Energy 179 (2019) 571–580, https://doi.org/10.1016/j.energy.2019.05.011.
[37] A.M. Abudour, S.A. Mohammad, K.A.M. Gasem, Modeling high-pressure phase equilibria of coalbed gases/water mixtures with the Peng–Robinson equation of state, Fluid Phase Equilib 319 (2012) 77–89, https://doi.org/10.1016/J.FLUID.2012.01.030.
[38] M.L. Huber, E.W. Lemmon, I.H. Bell, M.O. McLinden, The NIST REFPROP Database for Highly Accurate Properties of Industrially Important Fluids, Ind Eng Chem Res (2022), https://doi.org/10.1021/acs.iecr.2c01427.
[39] J. Szargut, D.R. Morris, F.R. Steward, Energy analysis of thermal, chemical, and metallurgical processes, (1988).
[40] W. Wagner, A. Pruß, The IAPWS Formulation 1995 for the Thermodynamic Properties of Ordinary Water Substance for General and Scientific Use, J Phys Chem Ref Data 31 (2002) 387, https://doi.org/10.1063/1.1461829.
[41] R. Span, W. Wagner, A New Equation of State for Carbon Dioxide Covering the Fluid Region from the Triple-Point Temperature to 1100 K at Pressures up to 800 MPa, J Phys Chem Ref Data 25 (2009) 1509, https://doi.org/10.1063/1.555991.
[42] R. Schmidt, W. Wagner, A new form of the equation of state for pure substances and its application to oxygen, Fluid Phase Equilib 19 (1985) 175–200, https://doi.org/10.1016/0378-3812(85)87016-3.
[43] U. Setzmann, W. Wagner, A New Equation of State and Tables of Thermodynamic Properties for Methane Covering the Range from the Melting Line to 625 K at Pressures up to 1000 MPa, J Phys Chem Ref Data 20 (2009) 1061, https://doi.org/10.1063/1.555898.
[44] E.W. Lemmon, R. Span, Short Fundamental Equations of State for 20 Industrial Fluids, J Chem Eng Data 51 (2006) 785–850, https://doi.org/10.1021/JE050186N.
[45] J.W. Leachman, R.T. Jacobsen, S.G. Penoncello, E.W. Lemmon, Fundamental Equations of State for Parahydrogen, Normal Hydrogen, and Orthohydrogen, J Phys Chem Ref Data 38 (2009) 721, https://doi.org/10.1063/1.3160306.
[46] O. Kunz, W. Wagner, The GERG-2008 wide-range equation of state for natural gases and other mixtures: An expansion of GERG-2004, J Chem Eng Data 57 (2012) 3032–3091, https://doi.org/10.1021/JE300655B/ASSET/IMAGES/MEDIUM/JE-2012-00655B_0029.GIF.
[47] D.R. Lide, CRC Handbook of Chemistry and Physics, 80th Edition,, 1999.
[48] P. Friedlingstein, M. O'Sullivan, M.W. Jones, R.M. Andrew, L. Gregor, J. Hauck, C. Le Quéré, I.T. Luijkx, A. Olsen, G.P. Peters, W. Peters, J. Pongratz, C. Schwingshackl, S. Sitch, J.G. Canadell, P. Ciais, R.B. Jackson, S.R. Alin, R. Alkama, A. Arneth, V.K. Arora, N.R. Bates, M. Becker, N. Bellouin, H.C. Bittig, L. Bopp, F. Chevallier, L.P. Chini, M. Cronin, W. Evans, S. Falk, R.A. Feely, T. Gasser, M. Gehlen, T. Gkritzalis, L. Gloege, G. Grassi, N. Gruber, Ö. Gürses, I. Harris, M. Hefner, R.A. Houghton, G.C. Hurtt, Y. Iida, T. Ilyina, A.K. Jain, A. Jersild, K. Kadono, E. Kato, D. Kennedy, K. Klein Goldewijk, J. Knauer, J.I. Korsbakken, P. Landschützer, N. Lefèvre, K. Lindsay, J. Liu, Z. Liu, G. Marland, N. Mayot, M.J. McGrath, N. Metzl, N.M. Monacci, D.R. Munro, S.-I. Nakaoka, Y. Niwa, K. O'Brien, T. Ono, P.I. Palmer, N. Pan, D. Pierrot, K. Pocock, B. Poulter, L. Resplandy, E. Robertson, C. Rödenbeck, C. Rodriguez, T.M. Rosan, J. Schwinger, R. Séférian, J.D. Shutler, I. Skjelvan, T. Steinhoff, Q. Sun, A.J. Sutton, C. Sweeney, S. Takao, T. Tanhua, P.P. Tans, X. Tian, H. Tian, B. Tilbrook, H. Tsujino, F. Tubiello, G.R. van

der Werf, A.P. Walker, R. Wanninkhof, C. Whitehead, A. Willstrand Wranne, R. Wright, W. Yuan, C. Yue, X. Yue, S. Zaehle, J. Zeng, B. Zheng, Global Carbon Budget 2022, Earth Syst Sci Data 14 (2022) 4811–4900. https://doi.org/10.5194/essd-14-4811-2022.
[49] S. Schneider, The worst-case scenario, Nature 458 (2009) 1104–1105, https://doi.org/10.1038/4581104a.
[50] R. Chodkiewicz, J. Porochnicki, B. Kaczan, Steam-gas condensing turbine system for power and heat generation, in, Proceedings of the ASME Turbo Expo (2001), https://doi.org/10.1115/2001-GT0097.
[51] R. Anderson, C. Hustad, P. Skutley, R. Hollis, Oxy-fuel turbo machinery development for energy intensive industrial applications, Energy Procedia 63 (2014) 511–523, https://doi.org/10.1016/j.egypro.2014.11.056.
[52] M.D. Butterworth, T.J. Sheer, High-pressure water as the driving fluid in an ejector refrigeration system, Appl Therm Eng 27 (2007) 2145–2152, https://doi.org/10.1016/J.APPLTHERMALENG.2005.07.011.
[53] A. Carotenuto, S. Di Fraia, N. Massarotti, S. Sobek, M.R. Uddin, L. Vanoli, S. Werle, Sewage Sludge Gasification Process Optimization for Combined Heat and Power Generation, Energies (basel) 16 (2023), https://doi.org/10.3390/en16124742.
[54] R.R. Bora, R.E. Richardson, F. You, Resource recovery and waste-to-energy from wastewater sludge via thermochemical conversion technologies in support of circular economy: a comprehensive review, BMC Chem. Eng. 2 (2020), https://doi.org/10.1186/s42480-020-00031-3.
[55] R.Y. Rubinstein, D.P. Kroese, Simulation and the Monte Carlo Method: Third Edition (2016), https://doi.org/10.1002/9781118631980.
[56] D. Xu, G. Lin, L. Liu, Y. Wang, Z. Jing, S. Wang, Comprehensive evaluation on product characteristics of fast hydrothermal liquefaction of sewage sludge at different temperatures, Energy 159 (2018) 686–695, https://doi.org/10.1016/J.ENERGY.2018.06.191.
[57] L. Qian, S. Wang, D. Xu, Y. Guo, X. Tang, L. Wang, Treatment of sewage sludge in supercritical water and evaluation of the combined process of supercritical water gasification and oxidation, Bioresour Technol 176 (2015) 218–224, https://doi.org/10.1016/J.BIORTECH.2014.10.125.
[58] L.F. Calvo, A.I. García, M. Otero, An Experimental Investigation of Sewage Sludge Gasification in a Fluidized Bed Reactor, Scientific World Journal 2013 (2013) 479403, https://doi.org/10.1155/2013/479403.
[59] J. Zhou, S. Liu, N. Zhou, L. Fan, Y. Zhang, P. Peng, E. Anderson, K. Ding, Y. Wang, Y. Liu, P. Chen, R. Ruan, Development and application of a continuous fast microwave pyrolysis system for sewage sludge utilization, Bioresour Technol 256 (2018) 295–301, https://doi.org/10.1016/J.BIORTECH.2018.02.034.
[60] Q. Xie, P. Peng, S. Liu, M. Min, Y. Cheng, Y. Wan, Y. Li, X. Lin, Y. Liu, P. Chen, R. Ruan, Fast microwave-assisted catalytic pyrolysis of sewage sludge for bio-oil production, Bioresour Technol 172 (2014) 162–168, https://doi.org/10.1016/J.BIORTECH.2014.09.006.
[61] Y.F. Huang, C.H. Shih, P. Te Chiueh, S.L. Lo, Microwave co-pyrolysis of sewage sludge and rice straw, Energy 87 (2015) 638–644, https://doi.org/10.1016/J.ENERGY.2015.05.039.
[62] I. Fonts, M. Azuara, G. Gea, M.B. Murillo, Study of the pyrolysis liquids obtained from different sewage sludge, J Anal Appl Pyrolysis 85 (2009) 184–191, https://doi.org/10.1016/J.JAAP.2008.11.003.
[63] U. Lee, J. Dong, J.N. Chung, Experimental investigation of sewage sludge solid waste conversion to syngas using high temperature steam gasification, Energy Convers Manag 158 (2018) 430–436, https://doi.org/10.1016/J.ENCONMAN.2017.12.081.
[64] C. Freda, G. Cornacchia, A. Romanelli, V. Valerio, M. Grieco, Sewage sludge gasification in a bench scale rotary kiln, Fuel 212 (2018) 88–94, https://doi.org/10.1016/J.FUEL.2017.10.013.
[65] Y. Chen, L. Guo, W. Cao, H. Jin, S. Guo, X. Zhang, Hydrogen production by sewage sludge gasification in supercritical water with a fluidized bed reactor, Int J Hydrogen Energy 38 (2013) 12991–12999, https://doi.org/10.1016/J.IJHYDENE.2013.03.165.
[66] S. Chen, Z. Sun, Q. Zhang, J. Hu, W. Xiang, Steam gasification of sewage sludge with CaO as CO2 sorbent for hydrogen-rich syngas production, Biomass Bioenergy 107 (2017) 52–62, https://doi.org/10.1016/J.BIOMBIOE.2017.09.009.
[67] J. Alvarez, G. Lopez, M. Amutio, M. Artetxe, I. Barbarias, A. Arregi, J. Bilbao, M. Olazar, Characterization of the bio-oil obtained by fast pyrolysis of sewage sludge in a conical spouted bed reactor, Fuel Process. Technol. 149 (2016) 169–175, https://doi.org/10.1016/J.FUPROC.2016.04.015.
[68] L. Shen, D.K. Zhang, An experimental study of oil recovery from sewage sludge by low-temperature pyrolysis in a fluidised-bed☆, Fuel 82 (2003) 465–472, https://doi.org/10.1016/S0016-2361(02)00294-6.
[69] I. Fonts, A. Juan, G. Gea, M.B. Murillo, J.L. Sánchez, Sewage Sludge Pyrolysis in Fluidized Bed, 1: Influence of Operational Conditions on the Product Distribution, Ind Eng Chem Res 47 (2008) 5376–5385, https://doi.org/10.1021/IE7017788.
[70] T.N. Trinh, P.A. Jensen, D.J. Kim, N.O. Knudsen, H.R. Sørensen, Influence of the pyrolysis temperature on sewage sludge product distribution, bio-oil, and char properties, Energy Fuel 27 (2013) 1419–1427, https://doi.org/10.1021/EF301944R/SUPPL_FILE/EF301944R_SI_001.PDF.
[71] T. Kus, P. Madejski, Analysis of the multiphase flow with condensation in the two-phase ejector condenser using CFD modeling, J Energy Resour Technol 1 (2023) 1–48, https://doi.org/10.1115/1.4064195.
[72] K. Stasiak, P. Ziołkowski, D. Mikielewicz, Selected Aspects of Performance of Organic Rankine Cycles Incorporated Into Bioenergy With Carbon Capture and Storage Using Gasification of Sewage Sludge, Journal of Energy Resources Technology, Transactions of the ASME 146 (2024), https://doi.org/10.1115/1.4064196.
[73] X. Zheng, Z. Ying, B. Wang, C. Chen, Hydrogen and syngas production from municipal solid waste (MSW) gasification via reusing CO2, Appl Therm Eng 144 (2018) 242–247, https://doi.org/10.1016/J.APPLTHERMALENG.2018.08.058.
[74] M. Baratieri, P. Baggio, B. Bosio, M. Grigiante, G.A. Longo, The use of biomass syngas in IC engines and CCGT plants: A comparative analysis, Appl Therm Eng 29 (2009) 3309–3318, https://doi.org/10.1016/J.APPLTHERMALENG.2009.05.003.
[75] H. Vishwajeet, M. Pawlak-Kruczek, M. Baranowski, A. Czerep, K. Chorążyczewski, M. Krochmalny, P. Ostrycharczyk, P. Ziółkowski, T. Madejski, A. Mączka, T. Arora, L. Hardy, J. Niedzwiecki, D. Badur, Mikielewicz, Entrained Flow Plasma Gasification of Sewage Sludge– Proof-of-Concept and Fate of Inorganics, Energies (basel) 15 (2022) 1–14, https://doi.org/10.3390/en15051948.
[76] M. Amiri, P. Ziolkowski, K. Stasiak, D. Mikielewicz, Analysis of cyclone separator solutions depending on SEC outlet conditions in nCO2PP, 36th International Conference on Efficiency, Cost, Optimization, Simulation and Environmental Impact of Energy Systems, ECOS 2023 (2023) 436–447. https://doi.org/10.52202/069564-0040.